

Calcification and dissolution of test  $\text{CaCO}_3$  cause changes in the surface water carbonate system. Deep-water chemistry affects and is affected by the dissolution of tests (e.g., Berger and Piper 1972; Dittert et al. 1999). Thermodynamic dissolution of tests is evident below the calcite lysocline. Below the calcite compensation depth (CCD, Fig. 8.1) only minor proportions of calcite are preserved (Broecker and Peng 1982). However, dissolution of calcareous tests may occur even some distance above the calcite lysocline (Anderson and Sarmiento 1994; Schiebel 2002; Schiebel et al. 2007), possibly caused by the remineralization of organic matter, and decreasing pH within microenvironments (Milliman et al. 1999). On the other hand, tests may settle below the CCD because they sink faster than they are dissolved. Consequently, well-preserved calcareous tests may occur in sediments deposited below the CCD, although the quantitative composition of the thanatocoenosis (fossil tests contained in sea floor sediments over geological time periods) below the CCD may not display the original fauna. Supra-lysoclineal dissolution of tests in surface sediments may be caused by remineralization of organic matter and chemical conditions at the fluffy (Fig. 8.2) sediment-water interface (De Villiers 2005). In addition to changes in the faunal composition and test calcite budget, encrustation and dissolution affect the chemical composition, i.e. isotope and element ratios of

planktic foraminifer tests (e.g., Lohmann 1995; Van Raden et al. 2011).

In this chapter, an overview is given on how foraminifer tests and assemblages are affected by transportation and expatriation, dissolution, and encrustation during sedimentation, i.e. when settling through the water column and being embedded in the surface sediment. Upon the arrival of planktic foraminifer tests at surface sediments taphonomic processes take over (e.g., Berger 1971; Lončarić et al. 2007).

---

## 8.1 Test Flux Dynamics

Planktic foraminifer assemblages in the water column and sea floor sediments represent the sum of production (i.e. population dynamics) and preservation (i.e. taphonomic processes) of tests, including transportation, dissolution and encrustation during sedimentation (e.g., Berger 1971; Vincent and Berger 1981; Schiebel 2002). In general, increased numbers of empty and sinking tests result from increased growth rates mostly in the surface waters. Maximum numbers of empty tests within the water column occur following time-intervals of maximum production such as, for example, in spring at mid-latitudes, and upwelling seasons in monsoon climates (Schiebel 2002). Following seasons of enhanced biological production in surface waters, a vast number of large and fast settling tests occur in

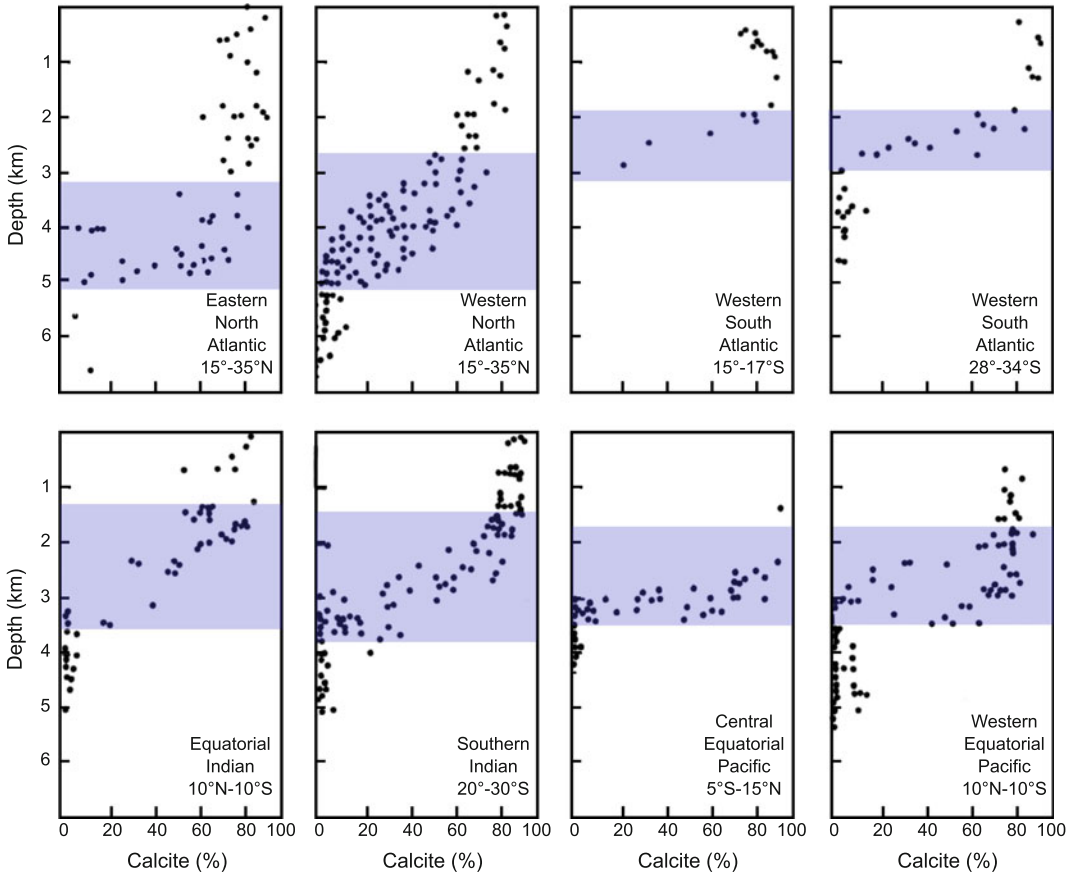


**Fig. 8.1** Calcite content in sea floor sediments indicating varying depths of calcite lysocline and calcite compensation depth (CCD) at the ocean-basin scale. Maximum calcite dissolution occurs between the lysocline (about 80 % calcite preservation) and the CCD (<20 % calcite

preservation). The upper limit of the depth-ranges shaded in blue gives the average depth of the lysocline, the lower limit gives the CCD. Deviations from the average result from regional effects. Redrawn from Broecker and Peng (1982). See also Sarmiento and Gruber (2006)



**Fig. 8.2** Planktic foraminifer tests in the fluffy sea floor sediment surface are exposed to physical and chemical processes, which may cause alteration of the shell. Fluffy layer on top of fine-grained sediment contained within

multicorer tube (left panel, width 4 cm). SEM image of fluffy sediment surface with planktic foraminifer tests (arrows) in the upper left corner (right panel, width 0.5 mm). Photo Ch. Hemleben

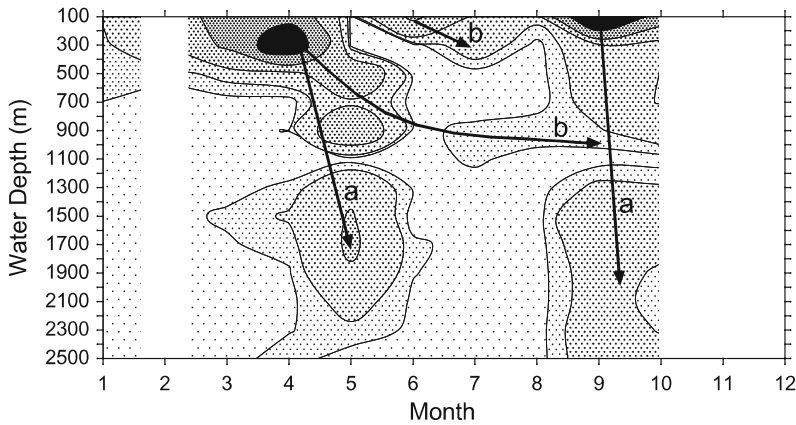


**Fig. 8.3** Schematic view of average monthly planktic foraminifer test calcite flux between 100 and 2500 m in the eastern North Atlantic around 47°N, 20°W. Settling tracks of fast (a) and slow (b) settling tests are indicated by arrows. The month of May was sampled over five

years. Black and gray levels correspond to  $\text{CaCO}_3$  flux  $>60$ ,  $>30\text{--}60$ ,  $>10\text{--}30$ ,  $>3\text{--}10$ ,  $>1\text{--}3$ , and  $<1$   $\text{mg m}^{-2}\text{d}^{-1}$ . Time-intervals without data coverage are shown in white. From Schiebel (2002)

the deep-water column (Schiebel 2002). At the same time, small tests become attached to larger particles and settle to depth. Differential settling velocities of planktic foraminifer tests result in different settling tracks (Fig. 8.3), which can be traced through the water column by repetitive sampling at the same location (time-series station).

Regional qualitative and quantitative discrepancies between fluxes are caused by differential production and preservation of tests. Discrepancies may be due to the better preservation of settling tests under low-oxygen conditions as, for example, within the oxygen minimum zone (OMZ) of the Arabian Sea (cf. Hermelin et al. 1992) in comparison to the well-oxygenated water column of the eastern North Atlantic. Although standing stocks in surface waters are similar at both sites during the SW monsoon and during spring, respectively, the number of empty tests in the deep water column in the Arabian Sea is much higher than in the eastern temperate North Atlantic (Schiebel 2002).

Assuming an average life expectancy of surface dwelling species of one month, assemblages of empty planktic foraminifer tests follow the seasonal production and sedimentation pattern (see Chap. 7). The settling community is composed mostly of empty tests, and includes

specimens that have undergone reproduction, and specimens, which died without having reproduced, mostly in juvenile and neanic stages. Following reproduction or death, planktic foraminifer tests sink out of their habitat and settle towards the sea floor (e.g., Berger 1971; Schiebel and Hemleben 2005). Planktic foraminifer tests settle to depth mostly individually in contrast to other particles like coccoliths, which are usually transported to depth within aggregates (e.g., Bishop et al. 1977; Thiel et al. 1989; Schiebel 2002; De La Rocha and Passow 2007; Schmidt et al. 2014). Settling velocities of individual tests depend on size, shape, and thickness of the shell, i.e., calcite mass (Fok-Pun and Komar 1983; Takahashi and Bé 1984). Small, thin-walled, and discoidal tests settle slower than large, heavy, and spherical tests (Table 8.1).

In addition to the empty test assemblage, cytoplasm-filled individuals, which may be alive but have lost buoyancy, are dragged to depth and contribute to the settling assemblage (Boltovskoy and Lena 1970; Takahashi and Bé 1984; Schiebel and Movellan 2012). Remaining cytoplasm within these tests has possibly no effect on their settling velocities (Table 8.2, Fig. 8.4). Spines decelerate the tests on their way to the sea floor by decreasing their weight-to-size ratio (Takahashi and Bé 1984; Furbish and Arnold 1997). In the

**Table 8.1** Settling velocity ( $\text{m day}^{-1}$ ) of empty planktic foraminifer tests calculated after Takahashi and Bé (1984)

Species	Sieve size ( $\mu\text{m}$ )							
	>100–125	>125–150	>150–200	>200–250	>250–315	>315–400	>400–500	>500
<i>T. quinqueloba</i>	100	115	142	–	–	–	–	–
<i>G. siphonifera</i>	107	167	196	334	361	373	639	–
<i>G. falconensis</i>	83	122	206	322	351	733	–	–
<i>G. bulloides</i>	83	115	237	328	434	597	885	1031
<i>G. scitula</i>	129	179	265	326	425	–	–	–
<i>G. glutinata</i>	100	185	247	359	476	–	–	–
<i>N. incompta</i>	91	129	222	408	493	–	–	–
<i>G. inflata</i>	100	173	232	350	515	738	1082	1534
<i>G. hirsuta</i>	122	167	296	441	691	986	1205	1551
Average	102	150	227	358	493	685	953	1339

From Schiebel and Hemleben (2000)

**Table 8.2** Average diameter, weight, and sinking speed determined from settling experiments of tests of selected non-spinose (first five species) and spinose planktic foraminifer species

P-specimens	n	Test diameter		Test weight		Sinking speed	
		( $\mu\text{m}$ )	$\pm$	( $\mu\text{g}$ )	$\pm$	( $\text{m day}^{-1}$ )	$\pm$
<i>G. menardii</i>	12	658	117	27	11	1104	228
<i>G. inflata</i>	10	234	45	4	2	504	91
<i>P. obliquiloculata</i>	13	391	72	14	8	796	362
<i>N. dutertrei</i>	12	458	93	16	8	842	290
<i>G. glutinata</i>	11	221	31	3	1	328	26
<i>O. universa</i>	8	573	74	8	6	277	144
<i>G. ruber</i>	10	314	49	6	3	198	94
<i>G. sacculifer</i>	11	328	99	10	6	274	143
<i>G. siphonifera</i>	10	377	96	5	4	271	191
<i>G. bulloides</i>	12	299	44	4	1	328	174
<b>A-specimens</b>							
<i>G. menardii</i>	15	572	174	22	15	918	322
<i>G. inflata</i>	11	309	101	9	8	753	311
<i>P. obliquiloculata</i>	9	399	71	13	11	769	333
<i>N. dutertrei</i>	14	374	94	11	7	766	359
<i>G. glutinata</i>	7	229	96	4	5	259	45
<i>O. universa</i>	8	521	52	17	7	701	219
<i>G. ruber</i>	22	289	82	8	6	723	321
<i>G. sacculifer</i>	16	430	170	25	20	1054	531
<i>G. siphonifera</i>	15	347	130	5	3	364	160
<i>G. bulloides</i>	11	211	28	1	1	208	46

All specimens are from plankton tow samples (P-specimens). A-specimens were treated in low temperature asher to remove organic matter, and some specimens did not lose all spines in settling experiments. After Takahashi and Bé (1984)

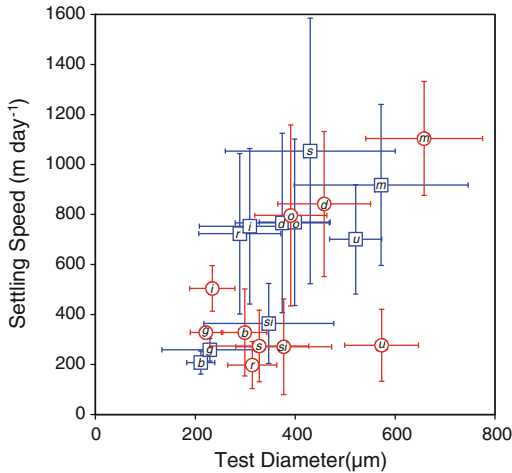


**Fig. 8.4** Test size ( $\mu\text{m}$ ) related settling speed ( $\text{m day}^{-1}$ ) of empty tests (blue) and cytoplasm bearing tests (red). Non-spinose species: *G. menardii* (m), *G. inflata* (i), *P. obliquiloculata* (o), *N. dutertrei* (d) and *G. glutinata* (g). Spinose species: *O. universa* (u), *G. ruber* (r), *G. sacculifer* (s), *G. siphonifera* (si), and *G. bulloides* (b). Settling velocities between originally spinose and non-spinose species, and cytoplasm bearing versus empty tests are not systematically different. Data from Takahashi and Bé (1984), see Table 8.2

general case where adult specimens had undergone gametogenesis, the spines would have been shed in surface waters. In addition, spines are particularly prone to dissolution due to their high surface-to-volume ratio, and rapidly dissolved after being shed or after death of the individual. Consequently, few spine-bearing tests occur in the subsurface water column. Subsurface dwelling species may increasingly contribute to the settling assemblage in the deeper water column. However, deep-dwelling species reproduce mostly in surface waters, and are included in the assemblage of empty tests within surface waters (Hemleben et al. 1987; Schiebel et al. 2002).

### 8.1.1 Accumulation of Tests Within the Water Column

Small tests settle through the water column more slowly than assumed from test size, weight, and drag coefficient alone (Fok-Pun and Komar 1983;

Takahashi and Bé 1984). In particular, tests of small and thin-shelled species like *T. quinqueloba* settle at low velocity and decelerate with depth due to increasing seawater viscosity. These light tests may come to a halt within the water column, and accumulate at interfaces of changing viscosity and density between different water bodies. Small and slow-sinking tests are particularly prone to accumulate in the mid water column. Mesobathyal assemblages of *T. quinqueloba* form, for example, during summer in the mid-latitude eastern North Atlantic, when low-productive conditions in surface waters allow accumulation of particles at density-interfaces in the mid water column (Fig. 8.3). Enhanced plankton production and consequently enhanced flux of settling matter during spring and fall causes scavenging of tests (cf. Honjo and Manganini 1993). Small tests, which had accumulated over the low productive summer season would be cleared out from the water column, and dragged to depths in spring and fall (Fig. 8.3).

**Viscosity and density:** The viscosity of a liquid may also be expressed as ‘fluidity’ or ‘thickness’. Less fluid means thicker and more viscose. The viscosity of seawater increases with salinity and decreases with temperature. In addition, viscosity increases with increasing pressure and depth. Temperature, salinity, and pressure affect (sea-) water density in the same sense as they affect viscosity, and buoyancy increases with increasing density. Since seawater is thicker and denser than freshwater, swimming in the sea is much easier for us (humans) than swimming in a lake. Hypersaline lakes like the Dead Sea even allow humans to float without much physical effort. Likewise, the viscosity and density of normal saline seawater supports buoyancy of live planktic foraminifers. In turn, active vertical displacement of planktic foraminifers by changing their buoyancy, via the amount of lipids embedded in vacuoles and fibrillar bodies

(i.e. cell organelles, which may act as floating bodies; Sect. 3.2.5), is impeded by the viscosity of ambient seawater.

Changes of viscosity and density of the mesobathyal water column in the subtropical to temperate North Atlantic are caused by the Mediterranean outflow water (MOW), in addition to the effect resulting from decreasing temperature. MOW is more saline than the adjacent Atlantic water bodies and spreads from Gibraltar to mid depths mostly to the west and north (cf. Van Aken 2000). MOW was repeatedly detected by CTD recording during sampling campaigns in summer at the same depths as test ‘clouds’ of small and thin-shelled *T. quinqueloba* (Fig. 8.3). One of those mesobathyal assemblages of empty tests composed mainly of small (100–125  $\mu\text{m}$ ) sized *T. quinqueloba* was sampled at 1000–1500 m water depth in the eastern North Atlantic in July and August 1992 at the upper limit of the MOW. A disproportionately large number of *T. quinqueloba* tests were also observed during September when the species constituted about 50 % of the assemblage sampled with a sediment trap (Schiebel 2002). In contrast, *T. quinqueloba* constitutes only 5–15 % of the live fauna in summer and fall in the eastern North Atlantic around 47°N, 20°W (Schiebel and Hemleben 2000) and about 10 % of the sea floor sediment assemblage at the same location (Prell et al. 1999). Ratios of *T. quinqueloba* tests much higher than 10 % are explained by an accumulation mechanism such as viscosity driven density separation.

Preservation of *T. quinqueloba* tests trapped at horizons of sharp density-changes in the mesobathyal water column has generally been good. Most of the tests show no signs of dissolution although being highly susceptible to dissolution (Table 8.3), despite long exposure times to ambient seawater of several weeks or months (Fig. 8.3). Above average preservation of tests is facilitated by the high calcite saturation state ( $\Omega > 1$ ) at 500–1500 m water depth in the North Atlantic (Schiebel et al. 2007), and even higher

calcite super-saturation of waters sourced from the western Mediterranean (Millero et al. 1979).

### 8.1.2 Pulsed Test Flux

Sedimentation of planktic foraminifer tests occurs in complex intermittent pulses (Fig. 8.5) rather than a steady flow (e.g., Sautter and Thunell 1989; Bijma et al. 1994; Peeters et al. 1999), resulting from ecological (e.g., food availability) and biological prerequisites (e.g., reproductive cycles). Pulsed flux events cause mass dumps of fast settling particles, and yield a major contribution of tests to the formation of deep-sea sediments (Sect. 8.5.2, Fig. 8.18). Mass dumps take place at regions and during periods of high biological productivity such as, for example, seasonal upwelling, spring blooms, and during fall (Kemp et al. 2000; Kawahata 2002; Schiebel 2002). During low productive periods, a steady rain of slow-sinking tests contributes only small amounts of tests to deep marine sediments (Schiebel 2002). In addition to seasonal test flux pulses, interannual changes affect different species to varying degrees, depending on their adaptation to regional ecologic conditions. Comparatively balanced flux occurs in the tropical ocean, and displays less distinct seasonality than at high latitudes. However, pulsed foraminifer test flux at low latitudes follows the same processes as at higher latitudes (Schiebel and Hemleben 2005; Buesseler et al. 2007). Seasonal and Interannual variability of species-specific flux patterns, and their relation to ecological conditions are determined by time-series analyses of samples (e.g., Lončarić et al. 2007; Wejnert et al. 2010; Kuhnt et al. 2013) (Sect. 10.1.8).

Quantitative differences between test (i.e. test numbers) and calcite (i.e.  $\text{CaCO}_3$  mass) fluxes result from differential production of species (environmental conditions and biological prerequisites), as well as differential flux modes. High settling velocities (Tables 8.1 and 8.2) of relatively large tests dominate the maximum  $\text{CaCO}_3$  flux pulses following maximum production of planktic foraminifers. In contrast, large numbers of small tests settle through the water

**Table 8.3** Ranking of average (Av., plus standard deviation,  $\pm$ ) dissolution susceptibility

Genus	Species	Av.	$\pm$	[1]	[2]	[3]
<i>Turborotalita</i>	<i>humilis</i>	<b>96</b>	6	100	100	89
<i>Globorotalia</i>	<i>tumida</i>	<b>90</b>	10	95	97	79
<i>Berggrenia</i>	<i>pumilio</i>	<b>89</b>	–	–	89	–
<i>Neogloboquadrina</i>	<i>pachyderma</i>	<b>88</b>	12	77	86	100
<i>Sphaeroidinella</i>	<i>dehiscens</i>	<b>87</b>	10	91	94	75
<i>Globorotalia</i>	<i>crassaformis</i>	<b>82</b>	5	86	77	82
<i>Pulleniatina</i>	<i>obliquiloculata</i>	<b>81</b>	10	82	91	71
<i>Neogloboquadrina</i>	<i>dutertrei</i>	<b>81</b>	7	73	83	86
<i>Globorotalia</i>	<i>inflata</i>	<b>78</b>	16	64	74	96
<i>Globorotalia</i>	<i>truncatulinoides</i>	<b>74</b>	17	59	71	93
<i>Globorotalia</i>	<i>menardii</i>	<b>68</b>	–	–	–	68
<i>Globorotalia</i>	<i>cavernula</i>	–	–	–	–	–
<i>Globorotalia</i>	<i>theyeri</i>	–	–	–	–	–
<i>Globorotalia</i>	<i>ungulata</i>	–	–	–	–	–
<i>Globoquadrina</i>	<i>conglomerata</i>	<b>65</b>	1	–	66	64
<i>Beella</i>	<i>digitata</i>	<b>62</b>	1	–	63	61
<i>Beella</i>	<i>megastoma</i>	–	–	–	–	–
<i>Globorotalia</i>	<i>hirsuta</i>	<b>62</b>	10	55	69	–
<i>Globorotaloides</i>	<i>hexagonus</i>	<b>60</b>	–	–	60	–
<i>Globorotalia</i>	<i>scitula</i>	<b>57</b>	0	–	57	57
<i>Candeina</i>	<i>nitida</i>	<b>51</b>	1	50	51	–
<i>Tenuitella</i>	<i>iota</i>	<b>50</b>	6	–	46	54
<i>Tenuitella</i>	<i>compressa</i>	–	–	–	–	–
<i>Tenuitella</i>	<i>fleisheri</i>	–	–	–	–	–
<i>Tenuitella</i>	<i>parkeriae</i>	–	–	–	–	–
<i>Globigerina</i>	<i>falconensis</i>	<b>46</b>	4	–	49	43
<i>Globigerinita</i>	<i>glutinata</i>	<b>46</b>	4	45	43	50
<i>Globigerinita</i>	<i>minuta</i>	–	–	v	–	–
<i>Globigerinella</i>	<i>calida</i>	<b>40</b>	8	–	34	46
<i>Globigerinita</i>	<i>uvula</i>	<b>40</b>	–	–	40	–
<i>Neogloboquadrina</i>	<i>incompta</i>	<b>37*</b>	–	–	–	–
<i>Orbulina</i>	<i>universa</i>	<b>34</b>	23	9	54	39
<i>Turborotalita</i>	<i>quinqueloba</i>	<b>32</b>	8	41	29	25
<i>Turborotalita</i>	<i>clarkei</i>	–	–	–	–	–
<i>Globigerinoides</i>	<i>conglobatus</i>	<b>30</b>	3	32	26	32
<i>Globigerina</i>	<i>bulloides</i>	<b>29</b>	8	36	31	21
<i>Globigerinoides</i>	<i>sacculifer</i>	<b>25</b>	3	23	23	29
<i>Globigerinella</i>	<i>siphonifera</i>	<b>22</b>	12	14	17	36
<i>Bolliella</i>	<i>adamsi</i>	<b>20</b>	–	–	20	–
<i>Globoturborotalita</i>	<i>tenella</i>	<b>20</b>	7	27	14	18

(continued)

**Table 8.3** (continued)

Genus	Species	Av.	±	[1]	[2]	[3]
<i>Globoturborotalita</i>	<i>rubescens</i>	<b>13</b>	4	18	11	11
<i>Globigerinoides</i>	<i>ruber</i> (white)	<b>9</b>	5	5	9	14
<i>Globigerinoides</i>	<i>ruber</i> (pink)	–	–	–	–	–
<i>Hastigerina</i>	<i>pelagica</i>	<b>4</b>	1	–	3	4
<i>Hastigerina</i>	<i>digitata</i>	–	–	–	–	–

High numbers correspond to high preservation potentials (after Dittert et al. 1999). Averages are calculated from data given by [1] Berger (1970), [2] Parker and Berger (1971), and [3] Berger (1979). Data\* on *N. incompta* (i.e. *N. pachyderma* subantarctic variety) are from Malmgren (1983). High standard deviation signifies species, which may produce shells of varying structure (e.g., pore density, thickness, GAM calcification). In case of missing data (e.g., *B. megastoma*), the respective species are related to other species of the same genus. No information is given on the ranking of *Dentigloborotalia anfracta*, *Gallitellia vivans*, *Orcadia riedeli*, *Streptochilus globigerus*, and *tenuitellids*

column at comparatively low velocity, and constitute low CaCO<sub>3</sub> flux during times of low production (cf. Deuser 1987). Both large and small tests predominantly result from time intervals of maximum production (Sect. 8.1.1). For example, maximum test flux at 2000 m water depth during summer in the NE Atlantic is mainly caused by small (20–125 µm in diameter) and thin-shelled tests of *T. quinqueloba* of relatively low calcite mass (Schiebel 2002), which were mainly produced in spring (cf. Schiebel and Hemleben 2000). Maximum test flux may hence cause only moderate CaCO<sub>3</sub> flux, and vice versa (Fig. 8.6).

### 8.1.3 Mass Sedimentation of Tests

Disproportionally high test-calcite flux of >1 g CaCO<sub>3</sub> m<sup>-2</sup>day<sup>-1</sup> at 1000–2500 m water depth occurred during March 1995 around new moon in the Arabian Sea (Schiebel 2002) (Sect. 8.5.1). The CaCO<sub>3</sub> flux pulse was mainly caused by large tests of *G. siphonifera* and *G. sacculifer* (>315–700 µm). Although *G. sacculifer* is a frequent faunal element in the Arabian Sea (Auras-Schudnagies et al. 1989; Conan and Brummer 2000; Naidu and Malmgren 1996), mass sedimentation of large tests of *G. sacculifer* was only observed in three (consecutive samples) out of 285 samples obtained in eight sampling campaigns (Schiebel 2002). Production and flux of *G. sacculifer* are related to the synodic lunar

cycle (Almogi-Labin 1984; Bijma et al. 1990a; Erez et al. 1991; Bijma et al. 1994). Consequently, the observed mass flux event does not represent the average sedimentation scenario, but is a monthly recurrent (though under-sampled) feature of deep marine sedimentation (cf. Anderson and Sarmiento 1994). Above-average ratios of large tests in low latitude sea floor sediments may be proof of these mass flux events (cf. Peeters et al. 1999). The temporal resolution of most deep sediment traps (>1000 m water depth) is too low to record single mass flux events. Shallow sediments traps (<1000 m depth) generally sample at low trapping efficiency (Scholten et al. 2001), and may miss mass flux events. Mass flux events may not be detected by most moored sediment traps, because mass flux over very short time-intervals of a couple of hours or days have been part of samples, which integrate over longer time-intervals of typically one or two weeks (see Sect. 10.1.7, Table 10.1). In contrast, the ratio of large to small tests obtained by multinet samples during mass flux events is much larger than in trap samples. Variations in standing stocks and fluxes are statistically significant for shorter time-intervals of hours rather than days. Unfortunately, mass flux events have rarely been sampled by plankton net-haul because their exact occurrence is unpredictable depending on ecological, biological, and hydrographical conditions, and wide dispersal of tests in the vastness of the deep ocean.

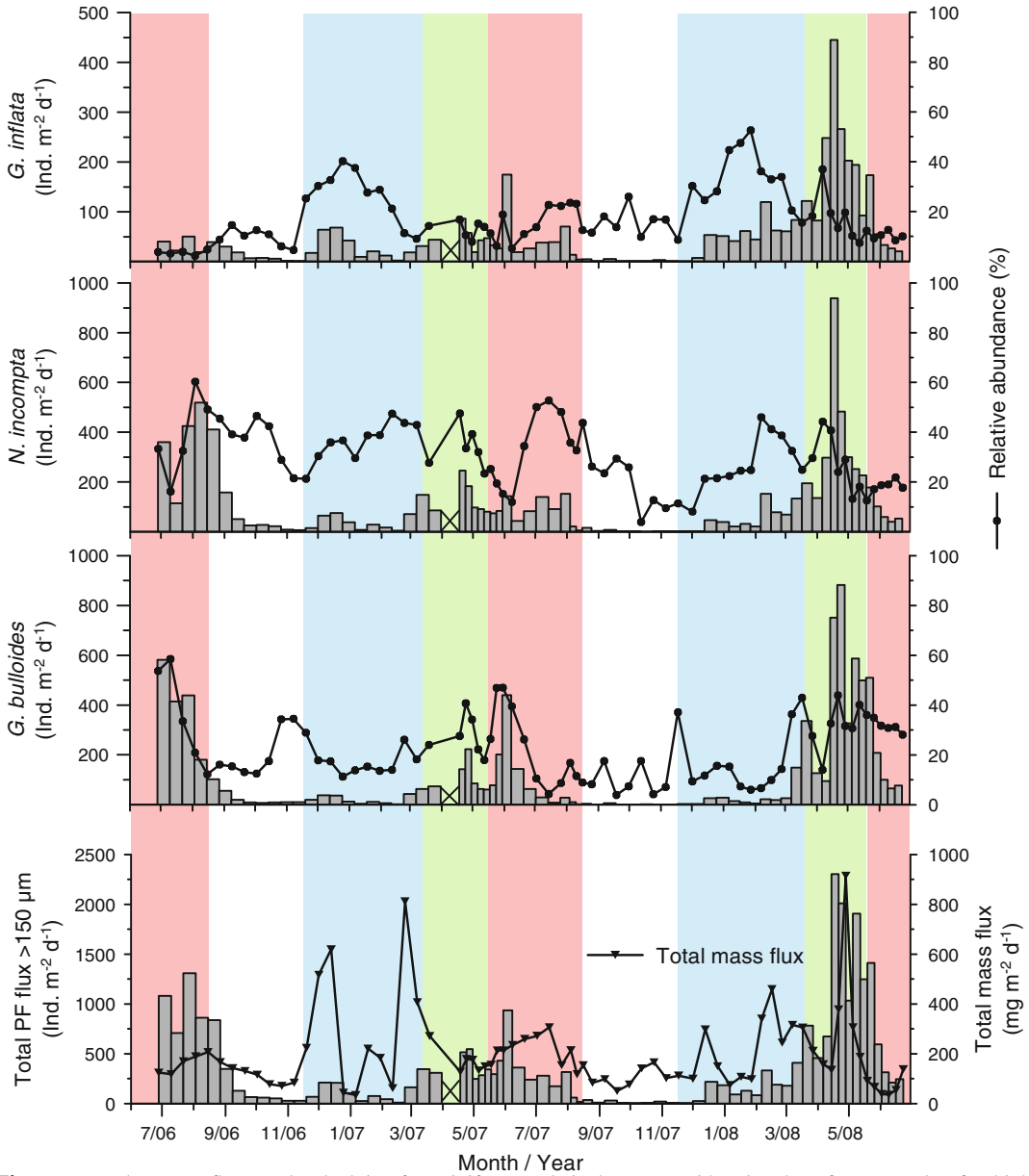
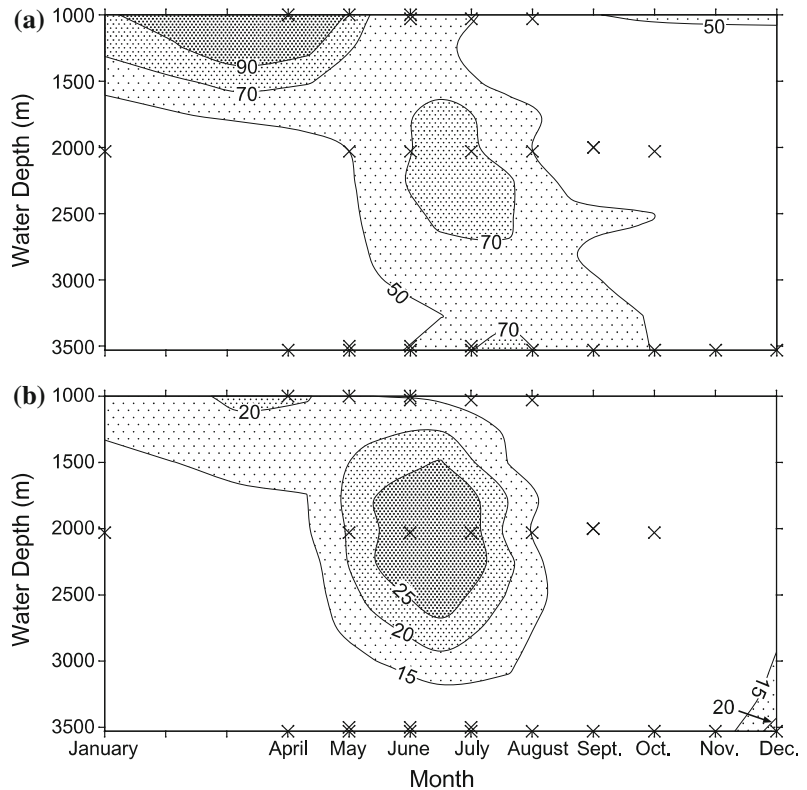


**Fig. 8.5** Total mass flux and planktic foraminifer (PF) test flux (gray bars) at the SE Bay of Biscay sampled with a sediment trap moored at 1700 m water depth from June 2006 to June 2008 (x-axis shows beginnings of the months). Fluxes of the most abundant species *G. bulloides*, *N. incompta*, and *G. inflata* are given as absolute and relative abundances (mean binomial standard errors of 3.8, 4.8 and 5 %, respectively). Maximum production and flux of planktic foraminifer

relatively occurs with a time lag of some weeks after high primary production (green) in spring. Time lags depend on species-specific settling modes and velocities (see Tables 8.1 and 8.2). Production in summer (red), fall (white), and winter (blue) is lower than in spring, and test flux occurs with a time lag of several weeks. Relative changes in seasonal production according to changes in sverdrup's critical depth (CRD) after Obata et al. (1996). 'X' indicates sampling gap. After Kuhnt et al. (2013)

**Fig. 8.6** **a** Planktic foraminifer  $\text{CaCO}_3$  flux ( $\text{mg m}^{-2}\text{day}^{-1}$ ), and **b** test flux ( $10^3 \text{ tests m}^{-2}\text{day}^{-1}$ ) sampled with sediment traps moored at  $47^\circ\text{N}$ ,  $20^\circ\text{W}$ , between 1000 m and 3530 m water depth. **a** Maximum  $\text{CaCO}_3$  mass flux in spring results from relatively few tests. In turn, **b** maximum test flux in summer is caused by high numbers of tests of low calcite mass. Crosses indicate sampling intervals. From Schiebel (2002)



### 8.1.4 The ‘Large Tests’ Phenomenon

Planktic foraminifer test assemblages deposited at the sea floor are biased towards large and fast sinking (up to  $1500 \text{ m d}^{-1}$ ) tests (e.g., Berelson 2002). In particular, sea floor sediments of the tropical to subtropical oceans contain disproportionately high numbers of large tests, when compared to the live fauna (Peeters et al. 1999). Those large tests may result from flux events like the mass sedimentation described above (Sect. 8.1.3). Pulsed flux events are a major contribution to deep-sea sediment accumulation and remove shell-bound bicarbonate over long time-scales from the upper ocean by transferring and burying it in deep-sea sediments (cf. Berger and Wefer 1990; Wefer 1989). Mass sedimentation requires the presence of species that have the biological prerequisites to form large tests and large numbers of specimens (Brummer et al. 1987; Hemleben et al. 1987; Caron et al. 1990) and are adapted to specific environmental conditions (Bijma et al. 1990b; Huber et al. 2000). In

addition to biological prerequisites, hydrographic conditions need to support mass dumps of large shells. One example is the fall dump of large diatoms in the Guaymas Basin, Gulf of California (Kemp et al. 2000), due to breakdown of stratification in the surface water column and sedimentation of an accumulated ‘shade flora’ in fall. A similar scenario is imaginable for planktic foraminifers.

In contrast to large tests, small tests are exposed to dissolution in the water column much longer than large tests due to their low sinking velocity (around  $100 \text{ m d}^{-1}$ ) and are preferentially removed from the assemblage when settling freely. The majority of small tests settle through the water column much slower than assessed from their test morphology (cf. Takahashi and Bé 1984). In turn, small tests can be quantitatively transported with good preservation from surface waters to depth during mass dump events along with other particles (Schiebel 2002), as observed from sediment trap samples from 2000 and 3000 m water depth below a naturally fertilized

high-nutrient low-chlorophyll (HNLC) region at Crozet seamount in the southern Indian Ocean (Salter et al. 2014). However, small tests are prone to winnowing, particularly by bottom water currents along bathymetric features like continental slopes, seamounts, and canyons (cf. Stow et al. 2002). To conclude, test assemblages result from a complex combination of biological, ecological, oceanographic, sedimentological, and taphonomic effects at the local to regional scale, favoring sedimentation of large tests over small tests with increasing water depth (cf. Berelson 2002).

---

## 8.2 Transportation and Expatriation

Horizontal transport and expatriation of live planktic foraminifers and empty tests by surface and subsurface currents adds complexity to the ecological and paleoceanographic analysis of faunas and assemblages (e.g., Weyl 1978). Ecologic conditions may change over the individual ontogenetic development and biogeochemical conditions, which affect calcite precipitation. Stable isotopes and Me/Ca ratios of the test calcite provide a mixed signal and do not necessarily display ecological conditions of the sampling location (Van Sebille et al. 2015). Transportation and expatriation of foraminifers within their ‘original water body’ (e.g., within an eddy) would not make analysis easier, because conditions at the sampling site would still not be displayed. The same is true for the transport of dead individuals and empty tests.

Depending on the velocity of surface and subsurface currents, planktic foraminifer tests are horizontally transported by up to several hundred kilometers. ‘Statistical funnels’ of a radius of up to ~500 km result from a modeling study of Siegel and Deuser (1997), using input data typical of small-sized and slow-sinking foraminifer tests (50–200 m day<sup>-1</sup>, see Tables 8.1 and 8.2), being affected by the Gulf Stream recirculation in the Sargasso Sea near Bermuda. For a sediment trap deployed at 1125 m water depth in the West Spitzbergen Current, average trajectory lengths of

25–50 km for *N. pachyderma* and 50–100 km for *T. quinqueloba* were calculated (von Gyldenfeldt et al. 2000). The reconstructed catchment areas are up to 230 km long and 140 km wide, i.e. catchment areas of 23,900 km<sup>2</sup> for tests of *N. pachyderma*, and 33,300 km<sup>2</sup> for tests of *T. quinqueloba* (Fig. 8.7). Both species are small sized and have long residence times in the water column. At current velocities of up to 40 cm s<sup>-1</sup> in the West Spitzbergen Current tests are transported over long distances and short time-intervals (von Gyldenfeldt et al. 2000). Since larger and heavier planktic foraminifer tests settle through the water column at higher velocity (Tables 8.1. and 8.2) they are transported over shorter distances of some tens of kilometers before arrival at depth. Therefore, larger tests provide results of higher regional accuracy, which is of particular importance when working in areas of high spatial variability such as hydrographic fronts and in regions which are characterized by high current velocities (cf. Caromel et al. 2013).

---

## 8.3 Dissolution

Dissolution of shells increases with decreasing carbonate ion concentration ( $[CO_3^{2-}]$ ) and calcite saturation state ( $\Omega$ ) at increasing water depth, and may continue at the sea floor sediment surface (e.g., Berger 1971; Henrich and Wefer 1986; Broecker and Clark 2001; De Villiers 2005; Schiebel et al. 2007). Increasing excess alkalinity (TA\*) below 3500–5000 m water depth may contribute to benthic carbonate dissolution (Berelson et al. 2007). In addition to carbonate chemistry of ambient seawater, the degree of dissolution is related to structure (i.e. dissolution susceptibility) of the foraminifer shell (Plate 8.1), as well as settling velocity and exposure time of tests (Schiebel et al. 2007).

In general, dissolution susceptibility is species-specific (Table 8.3), with *Hastigerina pelagica*, *Globigerinoides ruber*, and *Globoturbotalita rubescens* being most susceptible, and *Turbotalita humilis*, *Berggrenia pumilio*, encrusted *Neogloboquadrina pachyderma*, and

**Plate 8.1** Dissolution of planktic foraminifer shells illustrated with SEM images. (1) Well preserved assemblage with some mechanical damage only, and containing pteropod (P) shells made of aragonite. (2) Assemblage with well preserved planktic foraminifer shells, (3) moderate dissolution, and (4) heavy dissolution (S is *S. dehiscentis*). (5) Assemblage with near complete dissolution of calcareous shells, being dominated by agglutinated benthic foraminifer tests. (6) Loosening of layered shell structure, and peeling off of the inner calcite layers. (7) Labyrinth structures on the outer shell (left side), and peeling off of outer calcite layers (upper right corner). (8) Close-up of labyrinth structures on the outer shell. Bars of assemblages (1–5) 1 mm, close-ups (6, 7) 5  $\mu\text{m}$ , (8) 2  $\mu\text{m}$

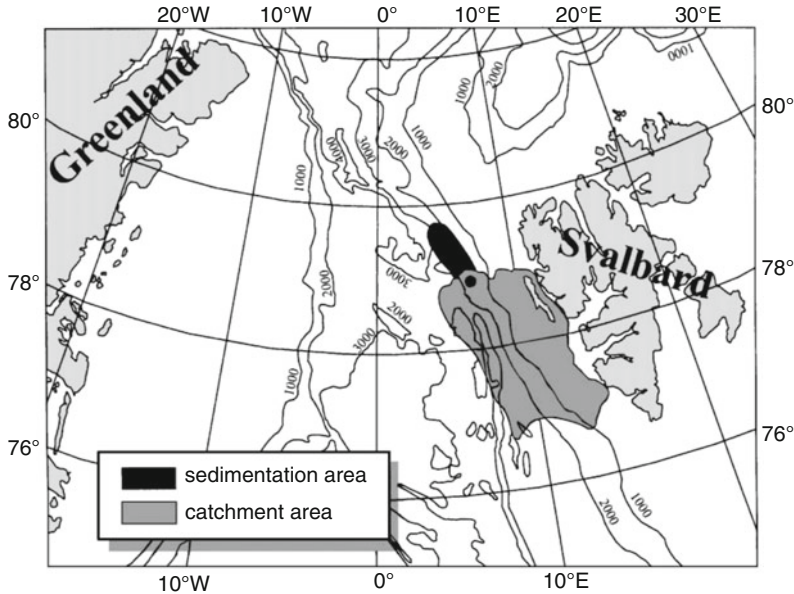
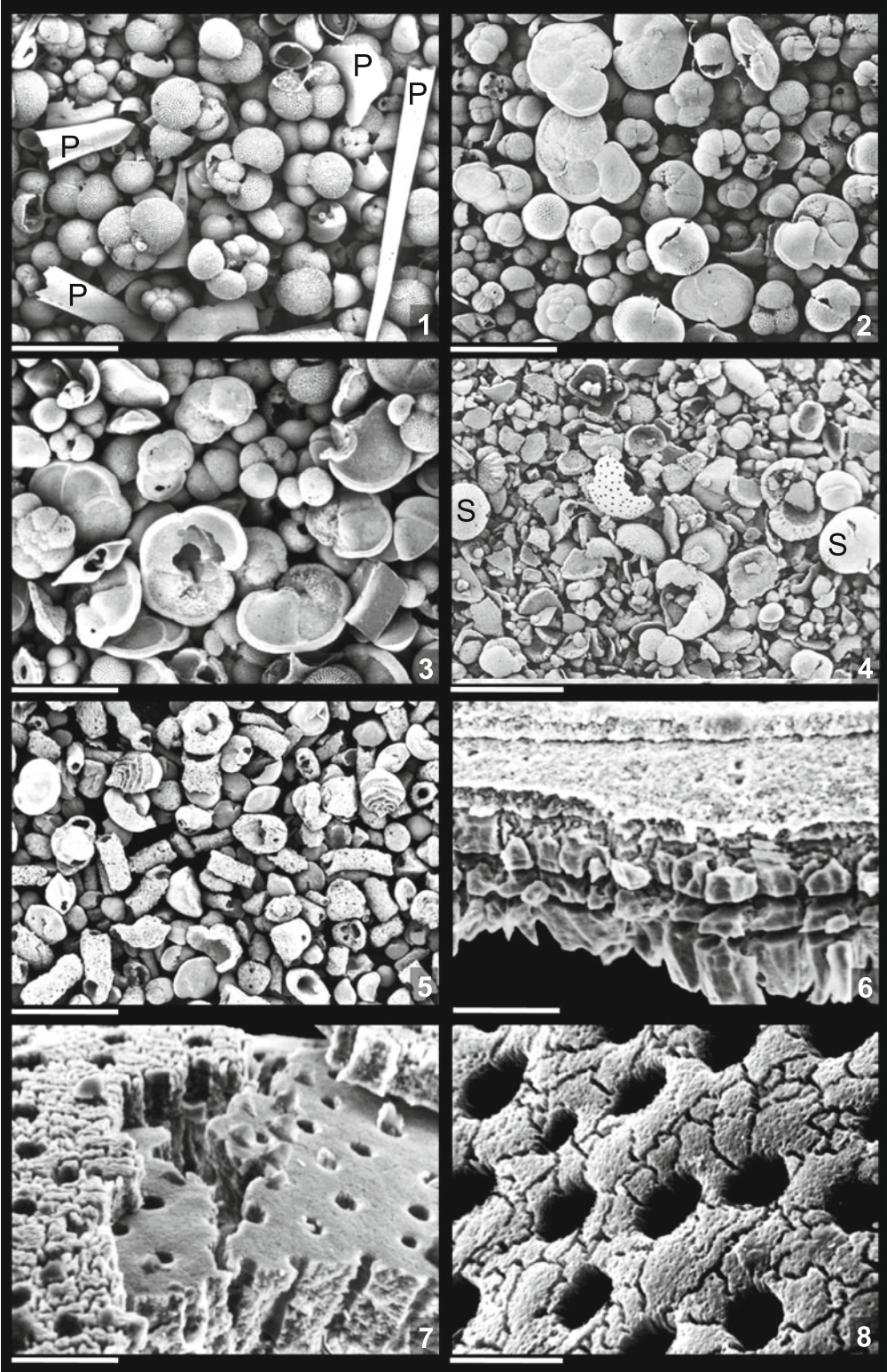


**Fig. 8.7** Catchment (gray) and sedimentation areas (black) calculated from assemblages of *T. quinqueloba* and *N. pachyderma*, sampled by a sediment trap moored in the West Spitzbergen current west of Svalbard. The solid black circle within the catchment area indicates the position of the mooring. The planktic foraminifer tests are

displaced largely from the SE to NW within the catchment area, and would (if not sampled by the sediment trap) be displaced further to the NW to finally be embedded within the surface sediment within the sedimentation area. After von Gyldenfeldt et al. (2000)

*Sphaeroidinella dehiscentis*, as well as some globorotalid species being most resistant to dissolution (see Dittert et al. 1999). Dissolution and destruction of the shell ultrastructure renders tests increasingly prone to fragmentation also by physical force. A fragmentation index is hence applied to the reconstruction of past  $[\text{CO}_3^{2-}]$  and  $\Omega$  at the basin scale (Berger 1973; Broecker and Clark 1999; Dittert and Henrich 2000; Conan et al. 2002; Volbers and Henrich 2002). In addition, preservation of planktic foraminifer tests varies at the regional and temporal scale and might be affected by biogeochemistry of ambient water and pH within microenvironments

(Milliman et al. 1999). On a global average, one fourth of the initially produced planktic foraminifer calcite is assumed to settle on the sea floor above the lysocline (Schiebel 2002). Dissolution-resistant species (e.g., *S. dehiscentis*, see Plate 8.1) increasingly dominate towards depth and may eventually constitute the residual test assemblages in deep basins (e.g., Ivanova et al. 2003). Starting at the lysocline to calcite compensation depth (CCD), the predominance of foraminifer calcite mass increasingly shifts towards a predominance of coccolithophore calcite mass in sediments below the CCD in subtropical gyres (Frenz et al. 2005), while coarser



particles (i.e. foraminifer tests and fragments) may dominate elsewhere (Paull et al. 1988). The phenomenon is caused by the fact that coccoliths are enveloped in organic matter and often embedded in fecal pellets, and are composed of purer and hence more dissolution resistant calcite than planktic foraminifers.

The most significant decrease in planktic foraminifer test flux occurs in the ocean's twilight zone at water depths between 100 and 1000 m (Fig. 8.8), and hence at depths of calcite supersaturation (Fig. 8.9) where thermodynamic calcite dissolution is unlikely (cf. Broecker and Peng 1982; Zeebe and Wolf-Gladrow 2001; Sarmiento

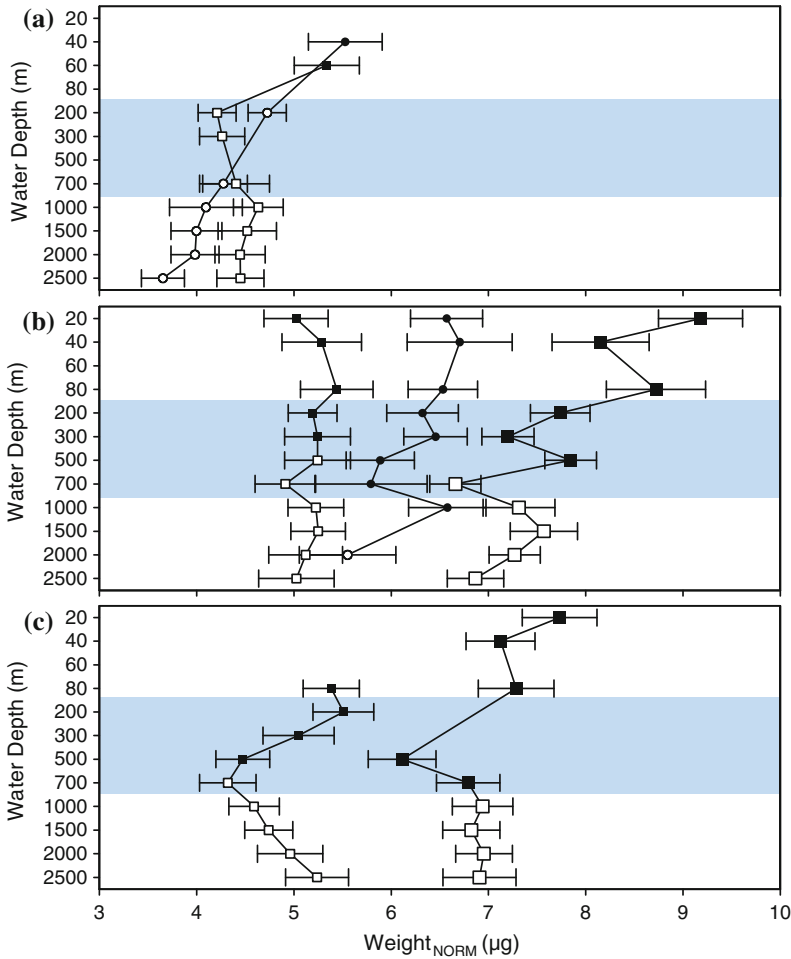


**Fig. 8.8** Size normalized test weight versus water depth, in the eastern North Atlantic **a** in spring 1992, and **b** in fall 1996 (47°N, 20°W), and **c** in the Arabian Sea (16°N, 60°E) during SW monsoon 1995. Although absolute test weight largely differs between species and ocean basins, maximum decrease in test weight uniformly occurs in the twilight zone (shaded) between about 100 and 1000 m water depth. Individual tests of *G. bulloides* and *G. glutinata* lose on average about one-fifth in weight while

settling through the twilight zone between about 100 and 1000 m water depth. Cytoplasm bearing tests are indicated by filled symbols, empty tests by open symbols. *Large squares* represent large *G. bulloides* (300 µm minimum test diameter), *small squares* represent small *G. bulloides* (250 µm), and *circles* represent small *G. glutinata* (250 µm). Standard deviation is given as error bars. From Schiebel et al. (2007)

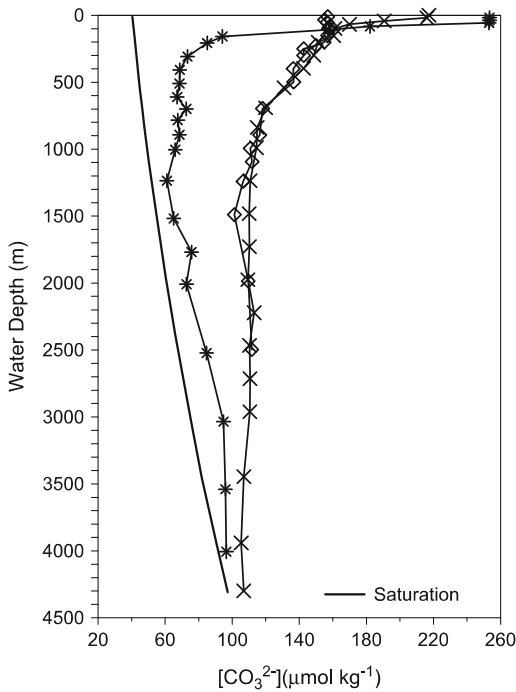


**Fig. 8.9** Carbonate ion concentration [ $\text{CO}_3^{2-}$ ] in the North Atlantic (47°N, 20°W) during spring (diamonds) and fall (crosses), and in the Arabian Sea (16°N, 60°E) during SW monsoon (asterisks) indicates calcite supersaturation throughout the analyzed water depths. From Schiebel et al. (2007)

and Gruber 2006; Friis et al. 2006; Schiebel et al. 2007). However, dissolution of planktic foraminifer calcite may not only be caused by the  $\Delta$  [ $\text{CO}_3^{2-}$ ] of ambient seawater at the outside of tests, and also takes place at the inside of tests. Dissolution at the inside of tests possibly results from bacterially mediated decomposition of cytoplasm and decreasing  $p\text{H}$  in microenvironments (Schiebel et al. 1997; Milliman et al. 1999; cf. also Boltovskoy and Lena 1970; Turley and Stutt 2000; Jansen et al. 2002). Dissolution of settling tests has been observed to be stronger in well-oxygenated waters than in low-oxygen environments where bacterial activity is limited by the availability of oxygen (e.g., Schiebel 2002). Accordingly, calcite preservation is better in the prominent oxygen minimum zone (OMZ) of the Arabian Sea than in well-oxygenated waters of the North Atlantic

(Fig. 8.9). In addition, better preservation of foraminifer tests in the Arabian Sea than in the NE Atlantic is probably due to higher average settling velocities of larger tests, and hence shorter exposure times of tests to ambient seawater in particular during seasonal (e.g., SW monsoon) mass flux events (Schiebel et al. 2007).

Below the twilight zone, at 1000–2500 m water depth, bacterially mediated dissolution has largely ceased [ $\text{CO}_3^{2-}$ ] and planktic foraminifer shell flux may increase to values higher than above (Figs. 8.8 and 8.9). Since mostly large and dissolution-resistant tests arrive at depths below the twilight zone, the average weight (i.e. calcite mass) and settling velocity of the remaining test assemblage increases with depth (Berelson 2002; Schiebel et al. 2007).

In addition to thermodynamic and bacterially mediated processes calcite dissolution far above the lysocline may take place within the guts of grazers (Hemleben et al. 1989; Jansen and Wolf-Gladrow 2001), but which is minor part of the global planktic foraminifer carbon turnover and calcite budgets (see Sect. 4.8 Predation). Quantitative dissolution of tests within fast sinking aggregates of marine snow is unlikely since planktic foraminifer tests are only occasionally contained within organic-rich and microbe-rich aggregates (cf. Ransom et al. 1998; Schmidt et al. 2014). To conclude, dissolution of planktic foraminifer tests in supersaturated waters with respect to calcite ( $\Omega > 1$ ) is hitherto not sufficiently explained and ‘the global carbonate budget is far from resolved’ (Berelson et al. 2007).

Dissolution and overgrowth of tests during sedimentation affect the composition of faunal assemblages through the presence or absence of tests of more or less dissolution-resistant species (e.g., Dittert et al. 1999). In the case of uncertain degrees of dissolution and overgrowth, care must be taken when analyzing biogeochemical data (i.e., stable isotopes, and element ratios) measured on planktic foraminifer tests (e.g., Pearson and Palmer 2000; Van Raden et al. 2011; Pearson 2012). Quantification of dissolution and its effect on the faunal composition of planktic foraminifer assemblages is difficult. Dissolution of

selected specimens can be visualized by scanning electron microscopy (SEM) or other high-resolution technology like computed tomography (CT; Johnstone et al. 2010). Since analyses of entire assemblages using SEM or CT would be too laborious, fragmentation indexes are employed for quantitative assessment of dissolution of samples (Plate 8.1). A fragmentation index for the evaluation of the effect of dissolution proposed by Ivanova (1988) relates the number of fragments (F) to the number of fragments plus entire tests (TE):

$$F = (F + TE) * 100 \quad (8.1)$$

The solution index (SI) of Berger (1973) relates the number of tests of resistant species (SR) to the total number of tests of common low latitude species (ST). When using the SI index of Berger (1973), the respective resistant and susceptible species need to be defined for a given region.

$$SI = SR/ST \quad (8.2)$$

## 8.4 Overgrowth

Overgrowth is due to non-biogenic processes. Dissolution and overgrowth of empty planktic foraminifer tests may affect tests settling through the water column (Deuser et al. 1981) and exposed to ambient seawater over days or weeks depending on their species-specific (test shape, shell surface and thickness) and size-related (i.e. test mass) settling velocity. Laboratory experiments have shown that various species form calcite crusts during their ontogeny (Hemleben et al. 1985). A massive calcite crust of disputed origin may cover tests of *N. pachyderma* from polar and sub-polar waters (Simstich et al. 2003) as well as other species at lower latitudes (Lohmann 1995). Deduced from the  $\delta^{18}\text{O}$  signal of *N. pachyderma* tests, Simstich et al. (2003) suggest active crust formation by the live foraminifer at sub-thermocline water depths between 70 and 250 m in the subpolar North Atlantic, whereas *T. quinqueloba* hardly forms any crust at the same

time. In contrast to the North Atlantic, calcite crusts have not been observed to the same extent in *N. pachyderma* tests from sediment-trap samples from 2000 and 3000 m water depth at subpolar waters near Crozet Seamount in the southern Indian Ocean (Salter et al. 2014). The questions arise as to what degree encrustation of *N. pachyderma* is affected by the chemistry (e.g.,  $[\text{CO}_3^{2-}]$ ) of ambient seawater at subsurface depths and to what degree calcite crusts of fossil tests of *N. pachyderma* in sea floor sediments are of biogenic or non-biogenic origin.

**Calcite crust:** Some uncertainty concerning the origin of calcite crusts covering planktic foraminifer shells may be due to inconsequent and confusing use of terminology. The formation of calcite crusts is sometimes attributed to ‘deep growth’. ‘Deep growth’ has been identified in species like *N. pachyderma* and is absent in other species as, for example, *G. ruber*. The term ‘deep growth’ might have been deduced from ‘overgrowth’, and does not refer to any biogenic process. Overgrowth is not engaged in active calcification of the individual shell and signifies purely thermodynamic calcite precipitation. Such calcite overgrowth on top of fossil shells is assumed precipitated in equilibrium with sediment chemistry and the chemistry of interstitial pore waters. Model calculations on the ratio of dissolution to encrustation of planktic foraminifer shells by Lohmann (1995) provide a theoretical explanation and quantification of the chemical composition, including stable isotopes, of planktic foraminifer tests from sediment samples (Fig. 8.10).

A positive  $\Delta\text{CO}_3^{2-}$  of surface and subsurface waters in the subpolar to temperate North Atlantic (Fig. 8.11) would foster thermodynamic calcite precipitation and encrustation of tests during sedimentation (cf. Simstich et al. 2003;

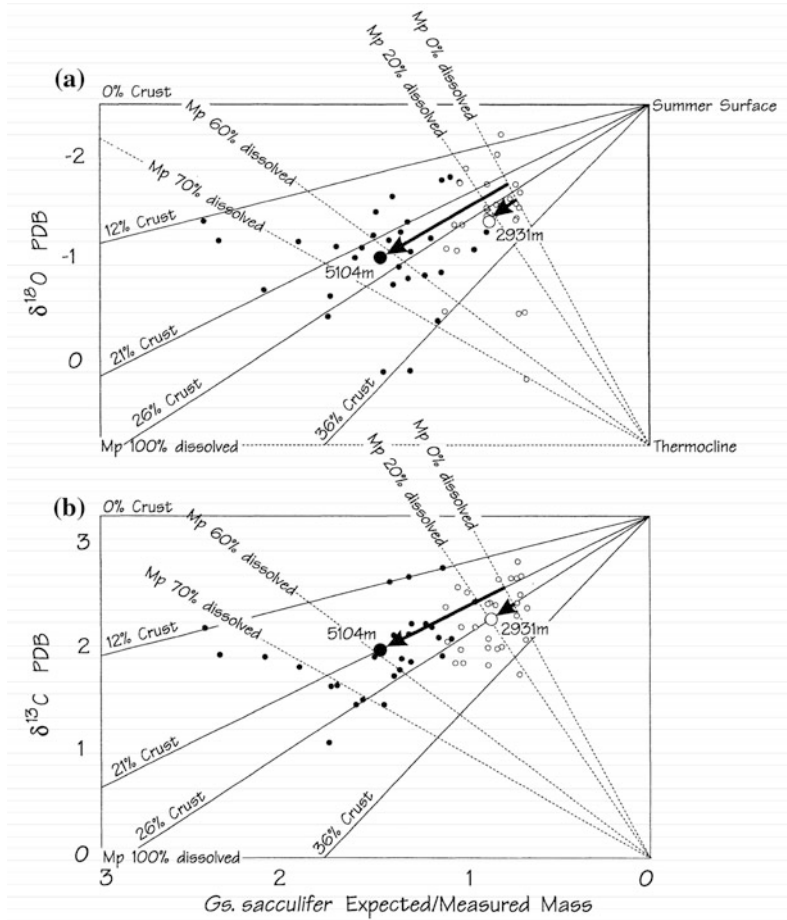


**Fig. 8.10** Changes in  $\delta^{18}\text{O}$  and  $\delta^{13}\text{C}$  of fossil *G. sacculifer* tests from surface sediment samples from the Sierra Leone Rise. *Solid dots* and *open circles* indicate samples from 5104 m and 2931 m water depth, respectively (large symbols indicate mean values). Degrees of

assumed encrustation and dissolution between the hypothetical end-members of ‘0 % Crust’ and ‘100 % dissolved’ are indicated by *solid* and *stippled lines*, respectively.  $M_p$  signifies the mass of primary chamber calcite. From Lohmann (1995)

Sarmiento and Gruber 2006, and references therein). In contrast, decreasing  $[\text{CO}_3^{2-}]$ , and negative  $\Delta\text{CO}_3^{2-}$  in the subsurface to deep water column would impede calcite precipitation and may cause dissolution of planktic foraminifer shells, which is the case in the tropical to temperate Atlantic (e.g., Broecker and Clark 1999;

Broecker and Clark 2001) and Southern Ocean (cf. Salter et al. 2014). In addition, low pH within microenvironments produced by degradation of organic tissues presumably causes considerable dissolution at the inside of tests (Milliman et al. 1999; Schiebel 2002; Schiebel et al. 2007; Johnstone et al. 2010; Constandache et al. 2013).

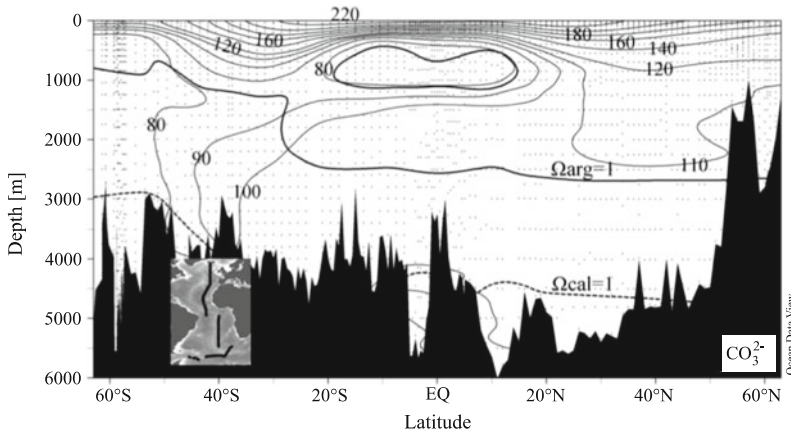


**Fig. 8.11** Vertical section of  $\Delta\text{DIC}_{\text{CaCO}_3}$  along transect from Iceland in the North Atlantic to the left, to the South Atlantic, along  $60^\circ\text{S}$  off the East Antarctic into the South Pacific, and along  $\sim 160^\circ\text{E}$  into the North Pacific off the Aleutian Islands. Super-saturation with respect to the mineral phases of aragonite (*hatched line*) and calcite (*solid line*) occurs above the saturation horizons,

$\Delta\text{CO}_3^{2-} = 0$ . Precipitation of  $\text{CaCO}_3$  and encrustation of tests fostered above and impeded below saturation horizon. Significant dissolution tends to coincide with the saturation horizon of aragonite. From Ocean Biogeochemical Dynamics by Jorge L. Sarmiento and Nicolas Gruber. Copyright (C) 2006 by Princeton University Press. Reprinted by permission

Dissolution at the sediment-water interface including the benthic fluff layer (see Fig. 8.2) above and within surface sediments depends on the residence time of tests and small-scale chemical conditions (cf. Lohmann 1995; De Villiers 2005; Feely et al. 2008). Dissolution or overgrowth of fossils tests within surface sediments act over much longer time scales, i.e. years to millennia, compared to days and weeks within the water column. As a result of long-term exposure to either carbonate super-saturation or under-saturation, overgrowth or dissolution of tests embedded in the sediment may appear less selective than in short-term processes within the water column. Precipitation of crusts affects tests embedded in calcareous surface sediments (Boussetta et al. 2011) and is a frequent phenomenon in supra-lysocline sediments (cf. Lohmann 1995; Van Raden et al. 2011). In contrast, little or no overgrowth occurs in clay-rich sediments and produces perfectly well preserved ('glassy') tests which provide ideal (uncontaminated) carriers of paleoceanographic proxies (Sexton et al. 2006). The fact that the

same species may or may not be encrusted in calcareous and clayey sediments, respectively, indicates potential formation of late sedimentary to early diagenetic overgrowth on top of fossil planktic foraminifer tests.

The combination of both dissolution and crust formation adds considerable uncertainty to the paleoceanographic interpretation of stable isotope data from fossil foraminifer calcite, which is difficult to disentangle and quantify. The long-known (e.g., Bouvier-Soumagnac et al. 1986) but often ignored combined signal of biogenic plus taphonomic effects needs to be quantified for detailed reconstruction of biological, ecological, and sedimentological processes, rather than information on average conditions resulting from analysis of the bulk test calcite. Data on bulk test calcite often foster the misleading idea that isotope and element ratios of bulk test calcite display the ecology, i.e. depth habitat and seasonal occurrence of any extinct species. When differentiating between primary (i.e. ontogenetic growth) and secondary (i.e. non-biogenic) calcite, the ecology and

taphonomy of a planktic foraminifer should be reconstructed in detail to provide accurate data on the paleoenvironment.

## 8.5 Carbon Turnover

Planktic foraminifers affect the regional to global carbon budget by sequestration of calcareous tests mainly from bicarbonate ( $\text{HCO}_3^-$ , ~90%), carbonate ( $\text{CO}_3^{2-}$ , ~10%), carbonic acid ( $\text{H}_2\text{CO}_3$ , ~1%), and carbon dioxide ( $\text{CO}_2$ , <1%) depending on  $p\text{H}$ , temperature, salinity, and concentration of dissolved inorganic carbon (DIC) of ambient seawater (e.g., Zeebe and Wolf-Gladrow 2001, Bjerrum plot). When precipitating their shell, planktic foraminifers fix half of the  $\text{CO}_2$  sourced from the different carbonate-species within their test calcite, and

release the other half to the environment (Fig. 8.12). Stoichiometrically, calcification of planktic foraminifer tests follows the equation  $\text{Ca}^{2+} + 2\text{HCO}_3^- \rightarrow \text{CaCO}_3 + \text{CO}_2 + \text{H}_2\text{O}$  (for bicarbonate only). Calcification of planktic foraminifer tests is hence a source of  $\text{CO}_2$  to surface waters and atmosphere, called carbonate counter pump, which acts on short time-intervals of days to seasons. On long geological time-scales of millions of years, sedimentation and burial of planktic foraminifer tests is a sink of  $\text{CO}_2$  (Zeebe 2012). Opposite to the carbon of planktic foraminifer tests, the carbon ingested with their food and stored in the foraminifer cytoplasm is quantitatively removed from the surface water carbon pool during sedimentation, and constitutes a sink of  $\text{CO}_2$  (Fig. 8.12).

Sedimentation of planktic foraminifers removes and transfers carbon from the surface to

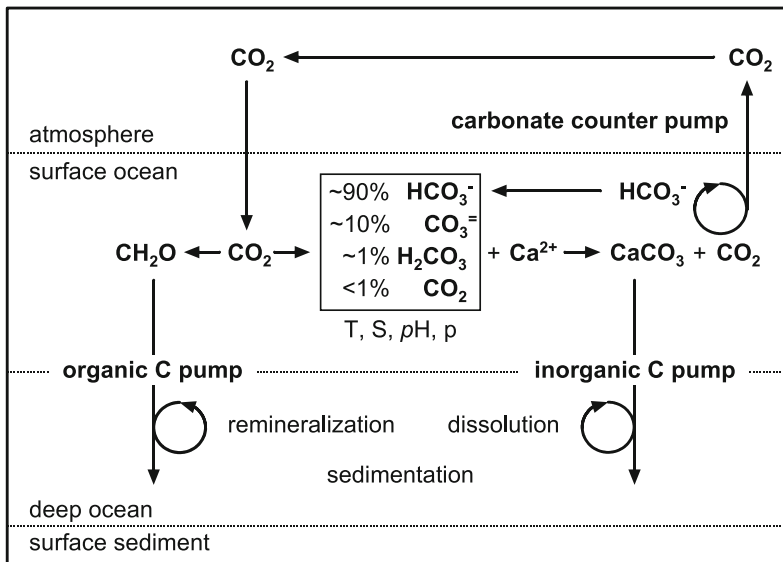


**Fig. 8.12** Non-stoichiometric scheme of the planktic foraminifer carbon pump, including the organic ( $\text{CH}_2\text{O}$ , i.e. cytoplasm carbon) and inorganic (test  $\text{CaCO}_3$ ) carbon mass. At a regional to global scale, the planktic foraminifer  $C_{\text{INORG}}$  to  $C_{\text{ORG}}$  ratio of settling assemblages ranges at about 5:1 to 10:1, whereas the  $C_{\text{INORG}}$  to  $C_{\text{ORG}}$  ratio of live individuals is ~1:3 (Schiebel and Movellan 2012). For one mole of  $\text{CaCO}_3$ -bound  $\text{CO}_2$ , one mole of  $\text{CO}_2$  is released into ambient seawater, and is recycled (round arrow) to  $\text{HCO}_3^-$  or released to the environment, i.e. the carbonate counter pump (e.g., Zeebe and

Wolf-Gladrow 2001). The ratio between the different carbonate species  $\text{HCO}_3^-$ ,  $\text{CO}_3^{2-}$ , and  $\text{H}_2\text{CO}_3$  involved in the formation of planktic foraminifer shell calcite depends on temperature (T), salinity (S),  $p\text{H}$ , pressure (p), and DIC concentration. Production of organic and inorganic matter occurs mainly in the surface mixed ocean. Remineralization and dissolution (round arrows) occurs primarily at mesobathyal depths and quantitatively affects sedimentation and  $\text{CO}_2$  burial. For absolute numbers on the organic and inorganic carbon pump see Schiebel and Movellan (2012) and Schiebel (2002), respectively

the deep water column where the carbon is temporarily withdrawn from ocean-to-atmosphere exchange for intermediate time-scales of decades to centuries, depending on upwelling dynamics and turnover rates of the global marine current systems (cf. Broecker 1987; Archer and Maier-Reimer 1994). When arriving at the sea floor, planktic foraminifer  $\text{CaCO}_3$  including the captured  $\text{CO}_2$  may be stored over long time-scales of millions of years depending on diagenetic effects and tectonic processes, and the preservation and dissolution of tests (e.g., Dittert et al. 1999; Broecker and Clark 1999; Broecker and Clark 2003).

**The biological carbon pump** in the ocean is the sum of processes, which affect the production, transportation, and remineralization of organic (e.g., cytoplasm) and dissolution of inorganic carbon (e.g., planktic foraminifer shell calcite). Planktic foraminifers affect the marine carbonate pump mainly through shell  $\text{CaCO}_3$  flux from surface waters towards surface sediments. The soft tissue pump (i.e. cytoplasm) concerns organic carbon, and has so far been regarded virtually non-existent in planktic foraminifers, because sedimentary planktic foraminifer tests are in general produced through reproduction, and settle to depth after having redistributed most cytoplasm to their offspring. In addition, planktic foraminifers have little effect on the efficiency of the biological carbon pump, since they are only minor part of ‘ballast’ in aggregates of particulate organic carbon (cf. De La Rocha and Passow 2007). However, planktic foraminifer soft tissue is systematically exported from surface waters to the sub-surface water column (cf. Boltovskoy and Lena 1970; Schiebel and Movellan 2012; Salter et al. 2014). Therefore, quantitative data on fossil planktic foraminifer assemblages could complement  $\delta^{13}\text{C}$  data as a proxy of the biological carbon pump of the

ancient oceans (e.g., Broecker 1971; Hilting et al. 2008).

Planktic foraminifer standing stocks and carbon turnover are highest in the surface mixed layer of the ocean, where  $\text{CO}_2$  exchange of ambient seawater is closely coupled to the atmospheric  $\text{CO}_2$  pool through diffusion at sub-seasonal time-scales. Live, i.e. cytoplasm bearing foraminifer individuals, which grow in surface waters may be mixed to depth by currents and surface water mixing, for example by eddies and during storms (Beckmann et al. 1987; Schiebel et al. 1995, cf. Koeve et al. 2002). On a global average, convection removes both calcite-carbon and cytoplasm-bound carbon at a ratio of  $\sim 10:1$ , respectively, from the atmosphere-coupled surface ocean to sub-surface depth (Schiebel and Movellan 2012). Planktic foraminifers thus contribute, although to a minor degree, to the marine biological carbon pump. Because their test size and calcite mass (Beer et al. 2010) are closely related to biomass (see Chap. 5, Fig. 5.4 on biomass) their calcite carbon to soft tissue carbon ratio may be used as proxy of the marine biological carbon pump (Movellan 2013).

### 8.5.1 Regional Calcite Budgets

Regional planktic foraminifer calcite flux ranges between  $<0.001$  and  $>2000 \text{ mg m}^{-2} \text{ d}^{-1}$  in oligotrophic, eutrophic, and mesotrophic waters (Fig. 8.13) of the global ocean (Schiebel 2002). Highest test calcite flux occurs at mid latitudes (Fig. 8.14, see also Žarić et al. 2006) caused by seasonally enhanced primary production and production of planktic foraminifers (Fig. 8.15). Data on shell  $\text{CaCO}_3$  flux span more than four orders of magnitude within water depth intervals between the surface ocean and 2500 m water depth (Fig. 8.13). Export production and flux of tests starts at the base of the surface mixed layer at about 100 m water depth (e.g., Koeve 2002).

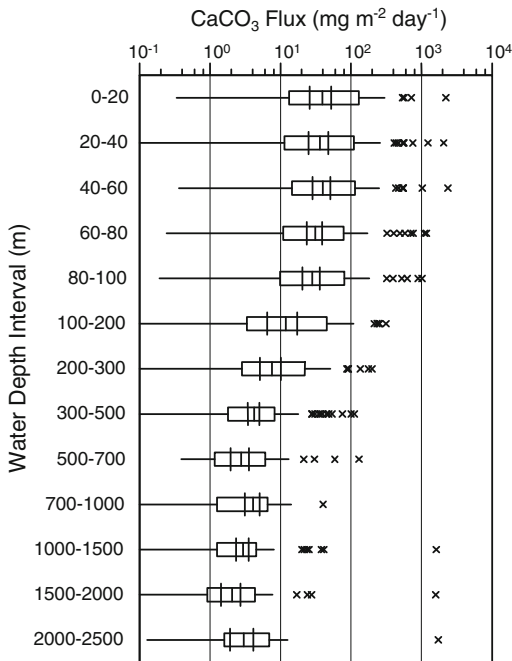


**Fig. 8.13** Average planktic foraminifer  $\text{CaCO}_3$  flux deduced from multinet samples from the North Atlantic, Arabian Sea, and Caribbean Sea ( $n = 1777$ ). Boxes cover the upper and lower quartile, with horizontal lines for the upper and lower adjacent values. Whereas the  $\text{CaCO}_3$  flux varies over five orders of magnitude, the average flux varies between the surface and mesobathyal water column decreases by only one order of magnitude over the twilight zone between 100 and 700 m water depth. The upper to lower quartile of fluxes between the sea surface and 200 m water depth exceeds one order of magnitude, indicating large variations in export production (e.g., Koeve 2002). Outliers (x) result from pulsed flux events following time-periods of enhanced production. Note that no outliers exist to the left of average distributions, indicating relatively constant ‘background’ (off-peak) test flux. Three extreme outliers between 1000 and 2500 m water depth result from mass flux events of *G. siphonifera* and *G. sacculifer* tests in the Arabian Sea. From Schiebel (2002)

The most significant decrease in flux takes place between 100 and 700 m depth. Changes in test  $\text{CaCO}_3$  flux between 700 and 2500 m are of minor amplitude (Figs. 8.13, 8.14 and 8.15).

Exceptionally high planktic foraminifer  $\text{CaCO}_3$  flux results from mass sedimentation of tests (see Sect. 8.1.3). Since mass flux events are episodic and rapid, they are rarely sampled by plankton net tows, and not detectable from sediment trap samples or surface sediments because of too low temporal sampling resolution.

Presence and absence of species with different biological prerequisites and ecological demands may exert a considerable effect on the flux of tests and  $\text{CaCO}_3$ . For example, very high planktic foraminifer  $\text{CaCO}_3$  flux  $>1000 \text{ mg m}^{-2} \text{ d}^{-1}$ , between 1000 and 2500 m (Fig. 8.13), was mainly caused by large specimens of *G. siphonifera* and *G. sacculifer* in the Arabian Sea in March 1995. The same is true for other seasonally pulsed  $\text{CaCO}_3$  flux peaks observed in the Arabian Sea in April and during August–September (see Sect. 8.1) (Schiebel 2002). Those flux peaks were caused by opportunistic species (*N. dutertrei*, *G. bulloides*), which proliferate during the late stages of the NE and SW monsoons, respectively. Test flux pulses (Tables 8.1 and 8.2) arrive at depths with the typical delay resulting from test-size related settling-velocity (cf. Takahashi and Bé 1984; Kroon and Ganssen 1989; Rixen et al. 2000; Schiebel and Hemleben 2000).

Moderate to low production and flux of planktic foraminifer tests and  $\text{CaCO}_3$  occurs in mesotrophic to oligotrophic waters of the temperate ocean and subtropical gyres (Fig. 8.14) and may be dominated by seasonal mass flux events in the same way as in eutrophic waters (e.g., Thunell and Honjo 1987) (see Sect. 8.1). Following mass flux events such as, for example, during the spring bloom in the NE Atlantic export flux decreases and flux pulses occur in the deeper water column. Maximum seasonality and sharp test flux peaks at high latitudes are caused by productivity during the short euphotic time-interval in summer (e.g., Fischer et al. 1988). In contrast, relatively balanced export flux, and steady sedimentation of tests in the tropical to subtropical ocean (Fig. 8.14, Caribbean; see also Sect. 7.2, Fig. 7.5) results from low seasonality compared to higher latitudes and year-round production and flux of foraminifer test calcite.

Low production and flux of planktic foraminifer tests occur in oligotrophic regions such as subtropical gyres (Fig. 8.14, Azores). However, seasonal test and  $\text{CaCO}_3$  flux peaks may also occur in oligotrophic waters. Distinct  $\text{CaCO}_3$  flux pulses at subsurface water depths in the subtropical gyre of the North Atlantic are, for

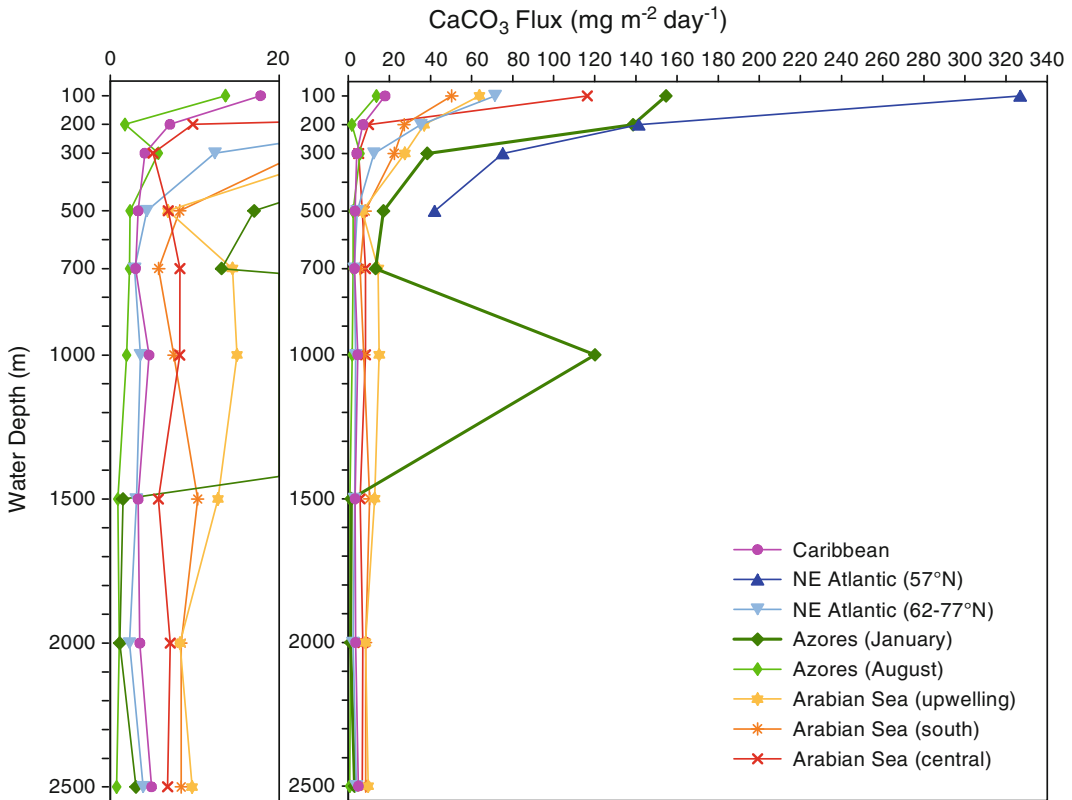


**Fig. 8.14** Monthly averages of regional planktic foraminifer CaCO<sub>3</sub> flux (mg m<sup>-2</sup>d<sup>-1</sup>) between 100 (export layer) and 2500 m water depth, calculated from plankton net samples (Schiebel 2002). High export flux occurs in mesotrophic and eutrophic regions such as in the NE Atlantic and Arabian Sea. Low export flux occurs in oligotrophic regions such as in the Caribbean Sea. The most significant decrease in flux takes place between 100

and 700 m water depth. Exceptionally high CaCO<sub>3</sub> flux at 100 m water depth in January in waters south of the Azores Islands was caused by reproduction and flux of large tests of *G. truncatulinoides*. Data are given for the lower level of each water depth interval. Left panel shows an enlarged view of low fluxes <20 mg m<sup>-2</sup>d<sup>-1</sup> given in right panel. From Schiebel (2002)

example, caused by *G. truncatulinoides*. After reproduction in surface waters during winter to early spring, the empty tests of adult *G. truncatulinoides* form a confined test-cloud settling through the subsurface water column (e.g., Deuser et al. 1981; Hemleben et al. 1987; Schiebel et al. 2002). Opposite to the flux of empty tests, live individuals of subsurface to deep-dwelling species in general contribute only a minor part to the foraminifer assemblage at subsurface depths, resulting from small standing stocks, which are dispersed over the vast expanses of the deep ocean (e.g., Lončarić et al. 2006).

## 8.5.2 Global Calcite Budget

The global planktic foraminifer calcite flux at 100 m water depth ( $F_{100}$ ) is estimated at 1.3–3.2 Gigatons (Gt, 10<sup>9</sup> tons) year<sup>-1</sup> (Fig. 8.16), equivalent to 23–56 % of the total open marine CaCO<sub>3</sub> particulate inorganic carbon (PIC) flux (Schiebel 2002). Test and calcite fluxes are calculated from the regional distribution of species obtained from net-tow (tests >100 μm in minimum diameter) and sediment trap samples and are assumed to cover most of the entire modern range of marine biogenic PIC flux (Schiebel 2002). During most of the year (off-peak periods), a large

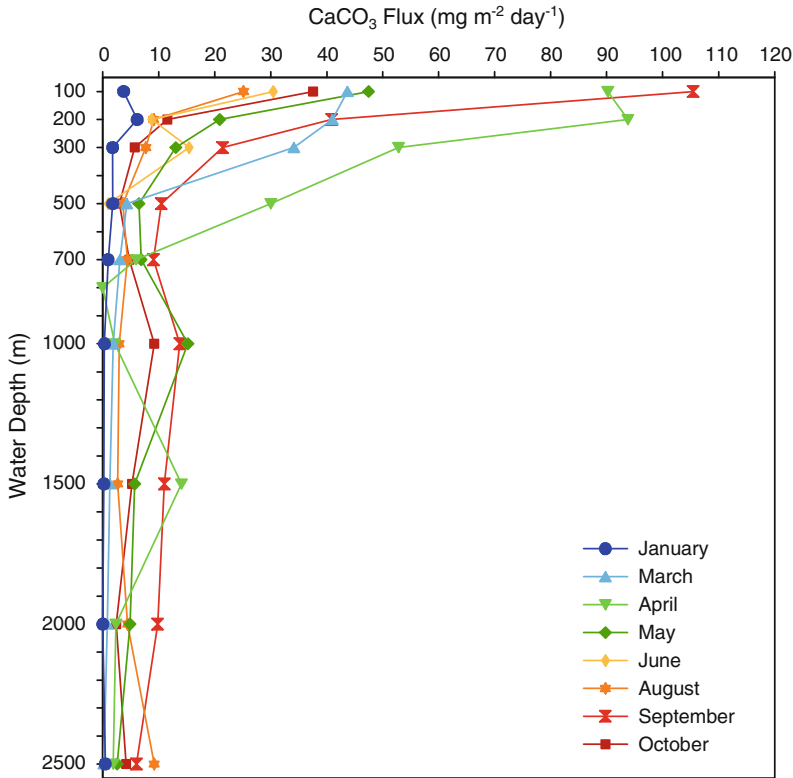


**Fig. 8.15** Average monthly planktic foraminifer  $\text{CaCO}_3$  flux in the temperate eastern North Atlantic around  $47^\circ\text{N}$ ,  $20^\circ\text{W}$  (BIOTRANS). Maximum decrease in  $\text{CaCO}_3$  flux occurs above 700 m water depths. Maximum export flux occurs in spring and fall. Test flux increase in deep waters below 700 m results from enhanced spring production and pulsed mass sedimentation in April and May. In

addition,  $\text{CaCO}_3$  flux is increasingly dominated by large and fast settling tests with high calcite mass at increasing water depth (Berelson 2002). In summer, small and slow settling tests cause low  $\text{CaCO}_3$  flux. Winter is characterized by low production and flux of planktic foraminifer  $\text{CaCO}_3$ . From Schiebel (2002)

part of the test calcite is dissolved while settling through the mesobathyal water column between 100–1000 m depth (Fig. 8.14).

As little as 1–3 % of the test  $\text{CaCO}_3$  initially exported from the surface mixed layer to sub-pycnocline waters may reach the above-lysocline seafloor on average (Schiebel 2002). Pulsed flux events, i.e. mass dumps of fast settling particles, yield a major contribution of tests to the formation of deep-sea sediments above the CCD. Highest flux and sedimentation rates of tests and calcite occur at latitudes between about  $30$ – $70^\circ$  (Fig. 8.17), where high and pointed spring production (spring bloom), and food supply coincides with high planktic

foraminifer diversity. The same applies to other regions of pointed seasonal production in the tropical to temperate ocean. On a global scale, about a quarter of the initially produced planktic foraminifer test  $\text{CaCO}_3$  settles on the sea floor and forms a major portion of sediment calcite above the calcite compensation depth, CCD (e.g., Berger 1971; Vincent and Berger 1981; Dittert et al. 1999; Schiebel 2002; Frenz et al. 2005).

The total planktic foraminifer contribution of  $\text{CaCO}_3$  to sediments above the CCD in the modern global ocean is estimated at  $0.36$ – $0.88 \text{ Gt yr}^{-1}$  (Fig. 8.18), which amounts to 32–80 % of the total marine sedimentary calcite budget (see also Archer 1996; Schiebel 2002;

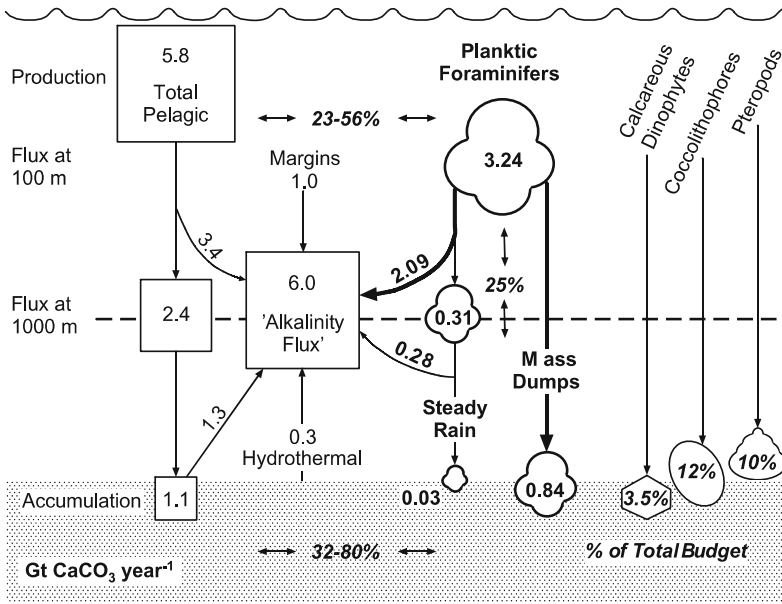


**Fig. 8.16** Global planktic foraminifer  $\text{CaCO}_3$  flux budget (center) in comparison with  $\text{CaCO}_3$  budgets given by Milliman et al. (1999, squares to the left). Planktic foraminifer shell calcite flux at 100 m depth is assumed equivalent to 23–56 % of the total open marine  $\text{CaCO}_3$  flux according to Milliman et al. (1999). An average of about 25 % of the initially produced planktic foraminifer  $\text{CaCO}_3$  is assumed to settle on the seafloor. The global

planktic foraminifer contribution of  $\text{CaCO}_3$  to marine sediments amounts to 32–80 % of the total above-CCD budget and is assumed  $\sim 1.1 \text{ Gt CaCO}_3 \text{ yr}^{-1}$ . An estimate of the coccolithophore, pteropod, and calcareous dinophyte contribution to the global open marine above-ACD (pteropods) and above-CCD  $\text{CaCO}_3$  accumulation is given to right. From Schiebel (2002)

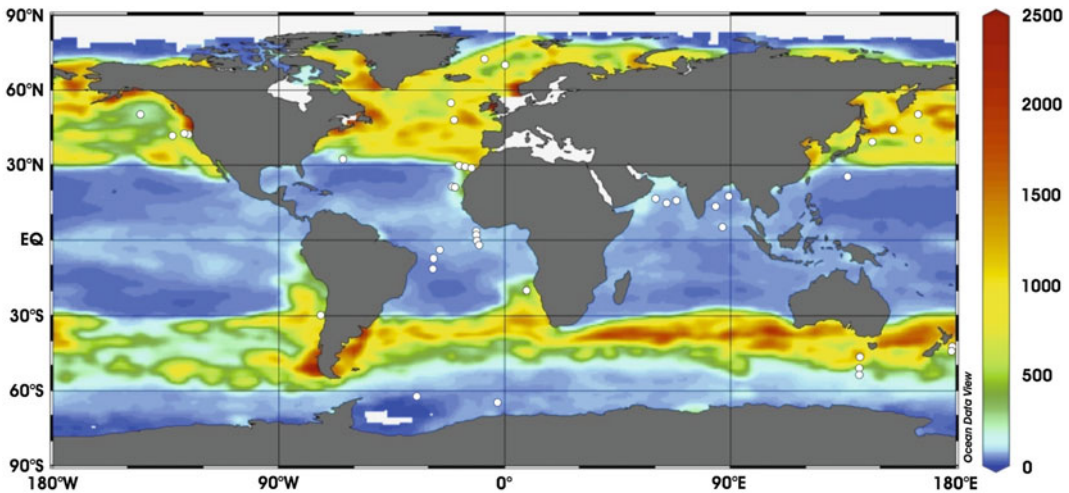


**Fig. 8.17** Modeled annual total foraminifer test flux ( $10^3$  individuals  $\text{m}^{-2}$ , for 18 species included in the empirical model) is highest from the subtropical to subpolar ocean of the northern and southern hemisphere. Circles mark positions of sediment traps comprised in the calibration data set. The general relative pattern of the global test flux is well represented by the model results. Many regional

patterns are not properly reproduced due to insufficient forcing by environmental parameters, and the correlation between primary production and planktic foraminifer test  $\text{CaCO}_3$  flux is weak (cf. Schiebel 2002). Absolute fluxes are assumed significantly underestimated in most cases. From Žarić et al. (2006)

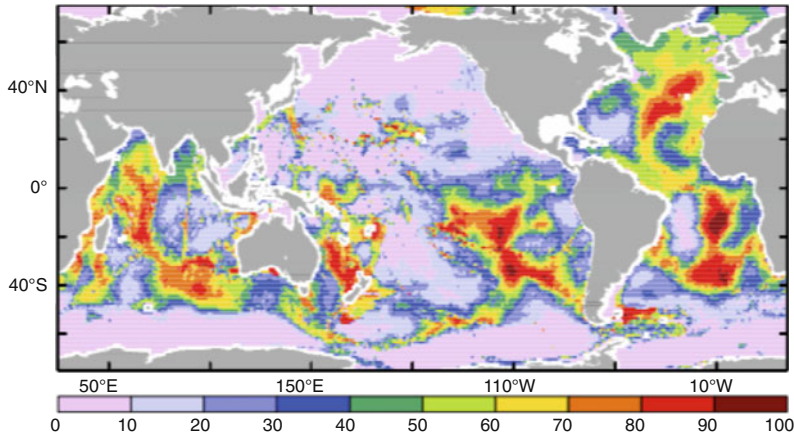


**Fig. 8.18** Map of the  $\text{CaCO}_3$  weight percent in the surface sediments. Low partial pressure of  $\text{CO}_2$  of young deep-water bodies in the Atlantic Ocean causes deep  $\text{CaCO}_3$  lysoclines and compensations depths, and results in well-preserved calcareous sediments of wide distribution. Oldest deep-water bodies of high  $p\text{CO}_2$  in the North Pacific cause shallow lysoclines and compensations

depths and ample carbonate dissolution. Accumulation of particles other than  $\text{CaCO}_3$  in the Southern Ocean results in dilution and carbonate-poor sediments, at relatively well preservation of calcareous shells. From Dunne et al. (2012). See also Sarmiento and Gruber (2006)

Sarmiento and Gruber 2006). The total accumulation of  $\text{CaCO}_3$  in the modern ocean is estimated at  $1.1 \text{ Gt yr}^{-1}$  (e.g., Milliman 1974; Milliman 1993; Milliman and Droxler 1996). In addition to planktic foraminifer  $\text{CaCO}_3$  flux, three major groups of calcareous plankton, i.e. coccolithophores, pteropods, and calcareous dinophytes add to the deep marine  $\text{CaCO}_3$  flux. Aragonite shells of pteropods are largely dissolved at the aragonite lysocline to aragonite compensation depth (ACD) above the calcite lysocline and CCD, respectively. Below the CCD, coccolithophore calcite takes over and increasingly constitutes the calcite fraction of abyssal sediment with increasing water depth and  $p\text{CO}_2$ , i.e. increasing  $p\text{H}$  (Frenz et al. 2005).

### 8.5.3 Global Biomass

In addition to the calcite-bound carbon of the tests, the global biomass (i.e. cytoplasm) of planktic foraminifers is estimated at  $\sim 8.5\text{--}32.7$  Teragrams (Tg, i.e.  $10^{12}$  g)  $\text{C yr}^{-1}$  including specimens  $>125 \mu\text{m}$  in diameter (Schiebel and

Movellan 2012). When adding juvenile and neanic specimens ( $<125 \mu\text{m}$  in tests size), the total planktic foraminifer biomass production is assumed as high as  $\sim 25\text{--}100 \text{ Tg C yr}^{-1}$  (i.e.,  $0.025\text{--}0.1$  Gigatons, Gt). The average global biomass-bound planktic foraminifer carbon would hence be four to six times less than the  $\text{CaCO}_3$  bound carbon of their test assemblages. The  $25\text{--}100 \text{ Tg}$  are estimated for a global ocean area of  $322 * 10^6 \text{ km}^2$  assumed to support planktic foraminifer production over nine months per year, accounting for three aphotic (winter) months without any significant production on a global average (Obata et al. 1996; Schiebel and Movellan 2012).

Assemblage biomass of planktic foraminifers varies by up to five orders of magnitude at intermediate water depth (100–700 m) and on average decreases by three orders of magnitude over 13 distinct water-depth intervals (see Methods Chap. 12) analyzed between the surface and deep water column at 2500 m depth (Fig. 8.19). Highest assemblage biomass in surface waters in the temperate North Atlantic and Arabian Sea is possibly biased by data from high-productive

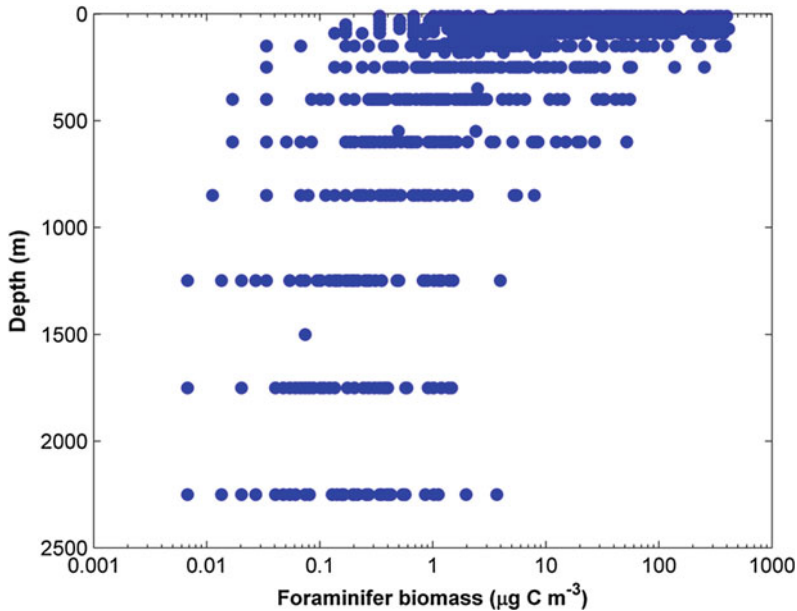


**Fig. 8.19** Log-normalised carbon-biomass ( $\text{Log}_{10} \mu\text{g m}^{-3}$ ) given for the total planktic foraminifer assemblage  $>125 \mu\text{m}$  (data available from <http://dx.doi.org/10.1594/PANGAEA.777386>). Data are calculated from average individual protein-biomass data and faunal

counts from the eastern North Atlantic Ocean, Caribbean Sea, and Arabian Sea ( $n = 1087$ , without zero values). All data given for the mid-points of the sampled water depth intervals. From Schiebel and Movellan (2012)

seasons, i.e. spring and SW monsoon in the Atlantic Ocean and Arabian Sea, respectively. Enhanced planktic foraminifer biomass in the Caribbean Sea, off Japan, and Oregon might be affected by land-derived input to the hemi-pelagic ocean, and effects on the primary and secondary production including planktic foraminifers. Low biomass in Red Sea waters is caused by oligotrophic conditions (Fig. 8.20). Biological production (including planktic foraminifers) in both Arctic and Antarctic waters has been assumed for time-intervals of only three months per year, and long aphotic polar seasons of nine months (Obata et al. 1996). However, Boetius et al. (2013) report significant under-ice primary production in the Arctic Ocean, which might also enhance the availability of food to planktic foraminifers. In conjunction with decreasing sea ice cover in the Arctic Ocean (e.g., Intergovernmental Panel on Climate Change 2007; Intergovernmental Panel on Climate Change 2013) primary production and secondary production, including planktic

foraminifers, may increase over the 21st century and beyond.

## 8.6 Summary and Concluding Remarks

The value of planktic foraminifers as proxy in paleoceanography and as part of the marine carbon turnover critically depends on the understanding of production and sedimentation of tests. Temporal scales of days to seasons, and regional sedimentation to basin scale transportation control the production of test assemblages (thanatocoenoses). Preservation and dissolution depend on thermodynamic ( $\Delta\text{CO}_3^{2-}$ ,  $\Omega$ ) and biological (often bacterially mediated processes) conditions.

Production and flux of planktic foraminifer test calcite affects, and is affected by, regional to global ocean carbon turnover. On short time-scales, test production is a source of  $\text{CO}_2$  to

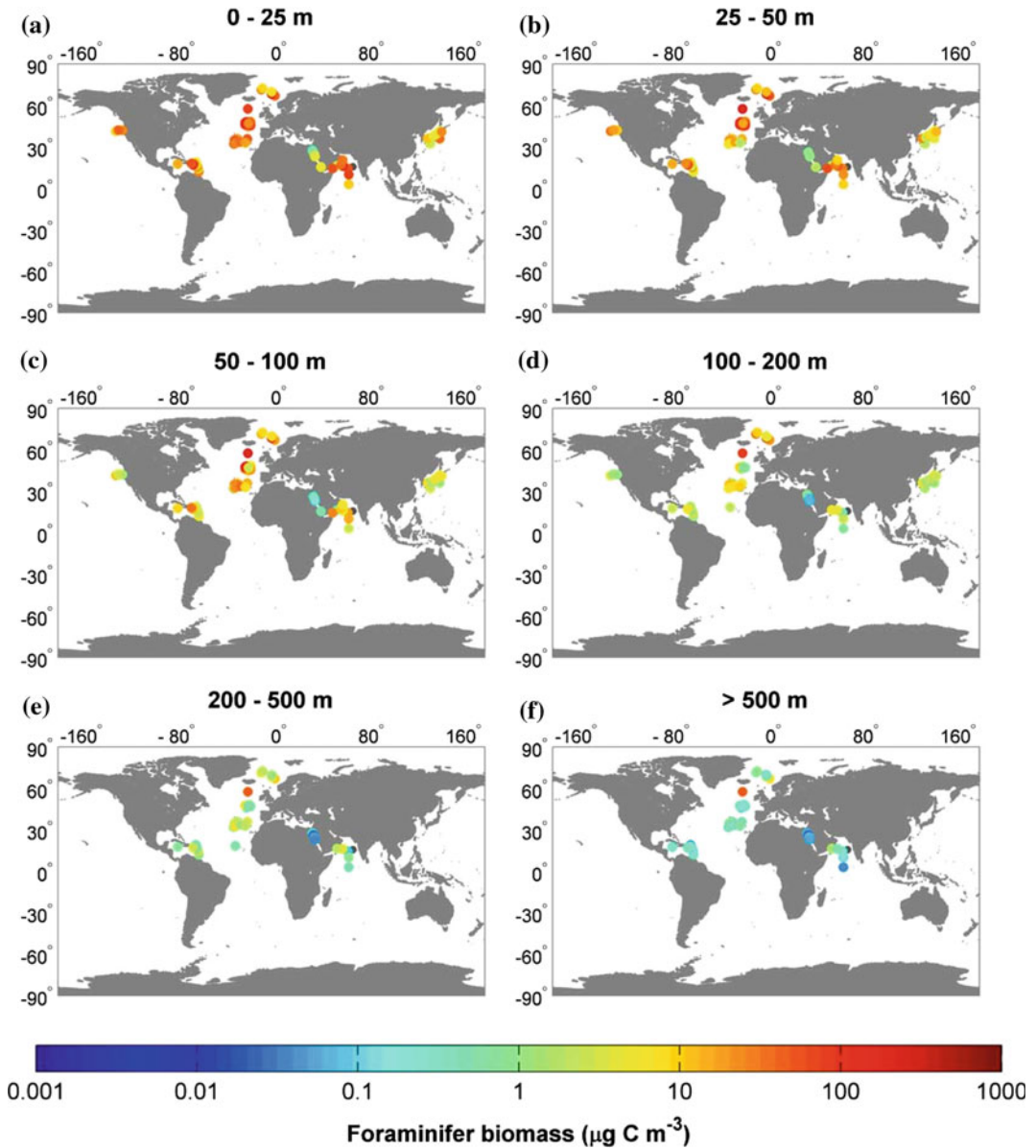


**Fig. 8.20** Log-normalised ( $\text{Log}_{10} \mu\text{g C m}^{-3}$ ) average depth related (a to f) planktic foraminifer assemblage biomass (PFAB) binned on a  $3^\circ \times 3^\circ$  grid, comprising the North Atlantic Ocean, Caribbean, Arabian Sea, Gulf

of Aden, Red Sea. Data on the eastern and western North Pacific Ocean off Oregon and Japan, respectively, are only on the upper 200 m of the water column. From Schiebel and Movellan (2012)

the ocean surface and lower atmosphere and acts as a sink of  $\text{CO}_2$  on long geological time scales. Sedimentation of organic carbon within foraminifer shells adds to the biological carbon

pump. Increasing  $[\text{CO}_2]$  and decreasing  $p\text{H}$  (ocean acidification, OA) are assumed to negatively affect calcification of planktic foraminifers. In analogy to past acidification events, planktic

foraminifers are assumed to buffer changes in  $pH$ . The buffering capacity of foraminifer shell formation on increasing  $[CO_2]$  and OA has not yet been quantified at the global scale. To date, calcification of planktic foraminifer tests is neither well constrained for the biological processes, nor for the quantitative effects on the marine carbon turnover. Future studies on the natural environment, as well as culture experiments (laboratory and mesocosm) should help to better understand planktic foraminifer calcification in a changing ocean and to calibrate new proxies for the reconstruction of the past marine carbon turnover.

Processes that affect sedimentation and dissolution are still insufficiently understood. This is partly owing to the fact that experimental approaches are limited by technological constraints. Smart chemostat experiments are needed to attain a better systematic understanding and quantification of small-scale to global processes, and to facilitate new modeling approaches. In addition, information on the natural environment is limited by methodological constraints like trapping efficiency of sediment traps. Concerted programs and sampling campaigns like the Joint Global Ocean Flux Study (JGOFS) was core project of the International Geosphere-Biosphere Programme (IGBP) (e.g., Ducklow and Harris 1993) and mesocosm experiments (e.g., Riebesell et al. 2013) enhance the systematic and quantitative understanding of mass fluxes. A combination of methods may provide a better qualitative and quantitative understanding of processes, which determine sedimentation and preservation versus dissolution of the planktic foraminifer shell calcite, i.e. the interplay of chemical, physical, and biological factors. Modern analytical methods will provide detailed information on ontogenetic shell calcite, and different kinds of calcite layers covering the pre-gametogenic planktic foraminifer shell. Those data are indispensable for a better understanding of carbon budgets and the use of planktic foraminifers as proxies in paleoceanography discussed in other chapters of this book.

## References

- Almogi-Labin A (1984) Population dynamics of planktic Foraminifera and Pteropoda—Gulf of Aqaba, Red Sea. *Proc K Ned Akad Van Wet Ser B Palaeontol Geol Phys Chem* 87:481–511
- Anderson LA, Sarmiento JL (1994) Redfield ratios of remineralization determined by nutrient data analysis. *Glob Biogeochem Cycles* 8:65–80. doi:10.1029/93GB03318
- Archer DE (1996) An atlas of the distribution of calcium carbonate in sediments of the deep sea. *Glob Biogeochem Cycles* 10:159–174. doi:10.1029/95GB03016
- Archer D, Maier-Reimer E (1994) Effect of deep-sea sedimentary calcite preservation on atmospheric  $CO_2$  concentration. *Nature* 367:260–263. doi:10.1038/367260a0
- Auras-Schudnagies A, Kroon D, Ganssen G, Hemleben C, van Hinte JE (1989) Distributional pattern of planktonic foraminifers and pteropods in surface waters and top core sediments of the Red Sea, and adjacent areas controlled by the monsoonal regime and other ecological factors. *Deep-Sea Res I* 36:1515–1533. doi:10.1016/0198-0149(89)90055-1
- Beckmann W, Auras A, Hemleben C (1987) Cyclonic cold-core eddy in the eastern North Atlantic. III *Zooplankton Mar Ecol Prog Ser* 39:165–173
- Beer CJ, Schiebel R, Wilson PA (2010) Technical note: on methodologies for determining the size-normalised weight of planktic Foraminifera. *Biogeosciences* 7:2193–2198. doi:10.5194/bg-7-2193-2010
- Berelson WM (2002) Particle settling rates increase with depth in the ocean. *Deep-Sea Res II* 49:237–251. doi:10.1016/S0967-0645(01)00102-3
- Berelson WM, Balch WM, Najjar R, Feely RA, Sabine C, Lee K (2007) Relating estimates of  $CaCO_3$  production, export, and dissolution in the water column to measurements of  $CaCO_3$  rain into sediment traps and dissolution on the sea floor: a revised global carbonate budget. *Glob Biogeochem Cycles*. doi:10.1029/2006GB002803
- Berger WH (1970) Planktonic Foraminifera: selective solution and the lysocline. *Mar Geol* 8:111–138. doi:10.1016/0025-3227(70)90001-0
- Berger WH (1971) Sedimentation of planktonic Foraminifera. *Mar Geol* 11:325–358. doi:10.1016/0025-3227(71)90035-1
- Berger WH (1973) Deep-sea carbonates: Pleistocene dissolution cycles. *J Foraminifer Res* 3:187–195. doi:10.2113/gsjfr.3.4.187
- Berger WH (1979) Preservation of Foraminifera. In: Lipps JH, Berger WH, Buzas MA, Douglas RG, Ross EH (eds) *Foraminiferal ecology and paleoecology*: Houston, Texas, Society of Economic Paleontologists and Mineralogists Short Course No 6, pp 105–155

- Berger WH, Piper DJW (1972) Planktonic Foraminifera: differential settling, dissolution, and redeposition. *Limnol Oceanogr* 17:275–287. doi:[10.4319/lo.1972.17.2.0275](https://doi.org/10.4319/lo.1972.17.2.0275)
- Berger WH, Wefer G (1990) Export production: seasonality and intermittency, and paleoceanographic implications. *Palaeogeogr Palaeoclimatol Palaeoecol* 89:245–254. doi:[10.1016/0031-0182\(90\)90065-F](https://doi.org/10.1016/0031-0182(90)90065-F)
- Bijma J, Erez J, Hemleben C (1990a) Lunar and semi-lunar reproductive cycles in some spinose planktonic foraminifers. *J Foraminifer Res* 20:117–127
- Bijma J, Faber WW, Hemleben C (1990b) Temperature and salinity limits for growth and survival of some planktonic foraminifers in laboratory cultures. *J Foraminifer Res* 20:95–116. doi:[10.2113/gsjfr.20.2.95](https://doi.org/10.2113/gsjfr.20.2.95)
- Bijma J, Hemleben C, Wellnitz K (1994) Lunar-influenced carbonate flux of the planktonic foraminifer *Globigerinoides sacculifer* (Brady) from the central Red Sea. *Deep-Sea Res I* 41:511–530. doi:[10.1016/0967-0637\(94\)90093-0](https://doi.org/10.1016/0967-0637(94)90093-0)
- Bishop JKB, Edmond JM, Ketten DR, Bacon MP, Silker WB (1977) The chemistry, biology, and vertical flux of particulate matter from the upper 400 m of the equatorial Atlantic Ocean. *Deep-Sea Res* 24:511–548. doi:[10.1016/0146-6291\(77\)90526-4](https://doi.org/10.1016/0146-6291(77)90526-4)
- Boetius A, Albrecht S, Bakker K, Bienhold C, Felden J, Fernández-Méndez M, Hendricks S, Katlein C, Lalande C, Krumpen T, Nicolaus M, Peeken I, Rabe B, Rogacheva A, Rybakova E, Somavilla R, Wenzhöfer F (2013) Export of algal biomass from the melting Arctic Sea ice. *Science* 339:1430–1432. doi:[10.1126/science.1231346](https://doi.org/10.1126/science.1231346)
- Boltovskoy E, Lena H (1970) On the decomposition of the protoplasm and the sinking velocity of the planktonic foraminifers. *Int Rev Gesamten Hydrobiol Hydrogr* 55:797–804. doi:[10.1002/iroh.19700550507](https://doi.org/10.1002/iroh.19700550507)
- Boussetta S, Bassinot F, Sabbatini A, Caillon N, Nouet J, Kallel N, Rebaubier H, Klinkhammer G, Labeyrie L (2011) Diagenetic Mg-rich calcite in Mediterranean sediments: quantification and impact on foraminiferal Mg/Ca thermometry. *Mar Geol* 280:195–204. doi:[10.1016/j.margeo.2010.12.011](https://doi.org/10.1016/j.margeo.2010.12.011)
- Bouvier-Soumagnac Y, Duplessy JC, Bé AWH (1986) Isotopic composition of a laboratory cultured planktonic foraminifer *O. universa*—implications for paleoclimatic reconstructions. *Oceanol Acta* 9:519–522
- Broecker WS (1971) A kinetic model for the chemical composition of sea water. *Quat Res* 1:188–207. doi:[10.1016/0033-5894\(71\)90041-X](https://doi.org/10.1016/0033-5894(71)90041-X)
- Broecker WS (1987) The biggest chill. *Nat Hist* 97:74–82
- Broecker WS, Clark E (1999) CaCO<sub>3</sub> size distribution: a paleocarbonate ion proxy? *Paleoceanography* 14:596–604. doi:[10.1029/1999PA900016](https://doi.org/10.1029/1999PA900016)
- Broecker WS, Clark E (2001) An evaluation of Lohmann's Foraminifera weight dissolution index. *Paleoceanography* 16:531–534. doi:[10.1029/2000PA000600](https://doi.org/10.1029/2000PA000600)
- Broecker WS, Clark E (2003) CaCO<sub>3</sub> dissolution in the deep sea: paced by insolation cycles. *Geochem Geophys Geosystems* 4:1059. doi:[10.1029/2002GC000450](https://doi.org/10.1029/2002GC000450)
- Broecker WS, Peng TH (1982) *Tracers in the sea*. Eldigio Press, New York
- Brummer GJA, Hemleben C, Spindler M (1987) Ontogeny of extant spinose planktonic Foraminifera (Globigerinidae): a concept exemplified by *Globigerinoides sacculifer* (Brady) and *G. ruber* (d'Orbigny). *Mar Micropaleontol* 12:357–381. doi:[10.1016/0377-8398\(87\)90028-4](https://doi.org/10.1016/0377-8398(87)90028-4)
- Buesseler KO, Lamborg CH, Boyd PW, Lam PJ, Trull TW, Bidigare RR, Bishop JKB, Casciotti KL, Dehairs F, Elskens M, Honda M, Karl DM, Siegel DA, Silver MW, Steinberg DK, Valdes J, Mooy BV, Wilson S (2007) Revisiting carbon flux through the ocean's twilight zone. *Science* 316:567–570. doi:[10.1126/science.1137959](https://doi.org/10.1126/science.1137959)
- Caromel AGM, Schmidt DN, Phillips JC (2013) Repercussions of differential settling on sediment assemblages and multi-proxy palaeo-reconstructions. *Biogeosciences Discuss* 10:6763–6781. doi:[10.5194/bgd-10-6763-2013](https://doi.org/10.5194/bgd-10-6763-2013)
- Caron DA, Roger Anderson O, Lindsey JL, Faber WW, Lin Lim EE (1990) Effects of gametogenesis on test structure and dissolution of some spinose planktonic Foraminifera and implications for test preservation. *Mar Micropaleontol* 16:93–116
- Conan SMH, Brummer GJA (2000) Fluxes of planktonic Foraminifera in response to monsoonal upwelling on the Somalia basin margin. *Deep-Sea Res II* 47:2207–2227
- Conan SMH, Ivanova EM, Brummer GJA (2002) Quantifying carbonate dissolution and calibration of foraminiferal dissolution indices in the Somali basin. *Mar Geol* 182:325–349. doi:[10.1016/S0025-3227\(01\)00238-9](https://doi.org/10.1016/S0025-3227(01)00238-9)
- Constandache M, Yerly F, Spezzaferri S (2013) Internal pore measurements on macroperforate planktonic Foraminifera as an alternative morphometric approach. *Swiss J Geosci* 106:179–186
- De La Rocha CL, Passow U (2007) Factors influencing the sinking of POC and the efficiency of the biological carbon pump. *Deep-Sea Res II* 54:639–658. doi:[10.1016/j.dsr2.2007.01.004](https://doi.org/10.1016/j.dsr2.2007.01.004)
- De Villiers S (2005) Foraminiferal shell-weight evidence for sedimentary calcite dissolution above the lysocline. *Deep-Sea Res I* 52:671–680. doi:[10.1016/j.dsr.2004.11.014](https://doi.org/10.1016/j.dsr.2004.11.014)
- Deuser WG (1987) Seasonal variations in isotopic composition and deep-water fluxes of the tests of perennially abundant planktonic Foraminifera of the Sargasso Sea: results from sediment-trap collections and their paleoceanographic significance. *J Foraminifer Res* 17:14–27
- Deuser WG, Ross EH, Hemleben C, Spindler M (1981) Seasonal changes in species composition, numbers, mass, size, and isotopic composition of planktonic Foraminifera settling into the deep Sargasso Sea. *Palaeogeogr Palaeoclimatol Palaeoecol* 33:103–127
- Dittert N, Henrich R (2000) Carbonate dissolution in the South Atlantic Ocean: evidence from ultrastructure

- breakdown in *Globigerina bulloides*. Deep-Sea Res I 47:603–620
- Dittert N, Baumann KH, Bickert T, Henrich R, Huber R, Kinkel H, Meggers H (1999) Carbonate dissolution in the deep-sea: methods, quantification and paleoceanographic application. In: Fischer G, Wefer G (eds) Use of proxies in paleoceanography. Springer, Berlin, pp 255–284
- Ducklow HW, Harris RP (1993) Introduction to the JGOFS North Atlantic bloom experiment. Deep-Sea Res II 40:1–8. doi:10.1016/0967-0645(93)90003-6
- Dunne JP, Hales B, Toggweiler JR (2012) Global calcite cycling constrained by sediment preservation controls. Glob Biogeochem Cycles 26. doi:10.1029/2010GB003935
- Erez J, Almogi-Labin A, Avraham S (1991) On the life history of planktonic Foraminifera: lunar reproduction cycle in *Globigerinoides sacculifer* (Brady). Paleoceanography 6:295–306
- Feely RA, Sabine CL, Hernandez-Ayon JM, Ianson D, Hales B (2008) Evidence for upwelling of corrosive “acidified” water onto the continental shelf. Science 320:1490–1492
- Fischer G, Fütterer D, Gersonde R, Honjo S, Ostermann D, Wefer G (1988) Seasonal variability of particle flux in the Weddell Sea and its relation to ice cover. Nature 335:426–428
- Fok-Pun L, Komar PD (1983) Settling velocities of planktonic Foraminifera: density variations and shape effects. J Foraminifer Res 13:60–68
- Frenz M, Baumann KH, Boeckel B, Höppner R, Henrich R (2005) Quantification of foraminifer and coccolith carbonate in South Atlantic surface sediments by means of carbonate grain-size distributions. J Sediment Res 75:464–475
- Friis K, Najjar RG, Follows MJ, Dutkiewicz S (2006) Possible overestimation of shallow-depth calcium carbonate dissolution in the ocean. Glob Biogeochem Cycles. doi:10.1029/2006GB002727
- Furbish DJ, Arnold AJ (1997) Hydrodynamic strategies in the morphological evolution of spinose planktonic Foraminifera. Geol Soc Am Bull 109:1055–1072. doi:10.1130/0016-7606(1997)109<1055:HSITME>2.3.CO;2
- Hemleben C, Spindler M, Breiting I, Deuser WG (1985) Field and laboratory studies on the ontogeny and ecology of some globorotaliid species from the Sargasso Sea off Bermuda. J Foraminifer Res 15:254–272
- Hemleben C, Spindler M, Breiting I, Ott R (1987) Morphological and physiological responses of *Globigerinoides sacculifer* (Brady) under varying laboratory conditions. Mar Micropaleontol 12:305–324
- Hemleben C, Spindler M, Anderson OR (1989) Modern planktonic Foraminifera. Springer, Berlin
- Henrich R, Wefer G (1986) Dissolution of biogenic carbonates: effects of skeletal structure. Mar Geol 71:341–362
- Hermelin JOR, Summerhays CP, Prell WS, Emeis KC (1992) Variations in the benthic foraminiferal fauna of the Arabian Sea: a response to changes in upwelling intensity? Upwelling systems: evolution since the early miocene. Geological Society, Special Publications, London, pp 151–166
- Hilting AK, Kump LR, Bralower TJ (2008) Variations in the oceanic vertical carbon isotope gradient and their implications for the Paleocene-Eocene biological pump. Paleoceanography. doi:10.1029/2007PA001458
- Honjo S, Manganini SJ (1993) Annual biogenic particle fluxes to the interior of the North Atlantic Ocean; studied at 34°N 21°W and 48°N 21°W. Deep-Sea Res II 40:587–607
- Huber R, Meggers H, Baumann KH, Henrich R (2000) Recent and Pleistocene carbonate dissolution in sediments of the Norwegian-Greenland Sea. Mar Geol 165:123–136. doi:10.1016/S0025-3227(99)00138-3
- Intergovernmental Panel on Climate Change (2007) Climate change 2007: synthesis report. Contribution of working groups I, II, and III to the fourth assessment report of the intergovernmental panel on climate change. IPCC, Geneva Switzerland
- Intergovernmental Panel on Climate Change (ed) (2013) Climate change 2013—The physical science basis: working group I contribution to the fifth assessment report of the intergovernmental panel on climate change. Cambridge University Press, Cambridge
- Ivanova EV (1988) Late quaternary paleoceanology of the Indian Ocean (based on planktonic foraminifers and pteropods). PP Shirshov Institute of Oceanology USSR Academy of Sciences, Moscow (in Russian)
- Ivanova E, Schiebel R, Singh AD, Schmiidl G, Niebler HS, Hemleben C (2003) Primary production in the Arabian Sea during the last 135,000 years. Palaeogeogr Palaeoclimatol Palaeoecol 197:61–82
- Jansen H, Wolf-Gladrow DA (2001) Carbonate dissolution in copepod guts: a numerical model. Mar Ecol Prog Ser 221:199–207
- Jansen H, Zeebe R, Wolf-Gladrow DA (2002) Modelling the dissolution of settling CaCO<sub>3</sub> in the ocean. Glob Biogeochem Cycles 16:1–16
- Johnstone HJH, Schulz M, Barker S, Elderfield H (2010) Inside story: an X-ray computed tomography method for assessing dissolution in the tests of planktonic Foraminifera. Mar Micropaleontol 77:58–70. doi:10.1016/j.marmicro.2010.07.004
- Kawahata H (2002) Suspended and settling particles in the Pacific. Deep-Sea Res II 49:5647–5664. doi:10.1016/S0967-0645(02)00216-3
- Kemp AES, Pike J, Pearce RB, Lange CB (2000) The “Fall dump”—a new perspective on the role of a “shade flora” in the annual cycle of diatom production and export flux. Deep-Sea Res II 47:2129–2154
- Koeve W (2002) Upper ocean carbon fluxes in the Atlantic Ocean: the importance of the POC:PIC ratio. Glob Biogeochem Cycles. doi:10.1029/2001GB001836
- Koeve W, Pollehne F, Oeschlies A, Zeitzschel B (2002) Storm-induced convective export of organic matter during spring in the northeast Atlantic Ocean.

- Deep-Sea Res I 49:1431–1444. doi:[10.1016/S0967-0637\(02\)00022-5](https://doi.org/10.1016/S0967-0637(02)00022-5)
- Kroon D, Ganssen G (1989) Northern Indian Ocean upwelling cells and the stable isotope composition of living planktonic foraminifers. *Deep-Sea Res I* 36:1219–1236
- Kuhnt T, Howa H, Schmidt S, Marié L, Schiebel R (2013) Flux dynamics of planktic foraminiferal tests in the south-eastern Bay of Biscay (northeast Atlantic margin). *J Mar Syst* 109–110:169–181. doi:[10.1016/j.jmarsys.2011.11.026](https://doi.org/10.1016/j.jmarsys.2011.11.026)
- Lohmann GP (1995) A model for variation in the chemistry of planktonic Foraminifera due to secondary calcification and selective dissolution. *Paleoceanography* 10:445–457
- Lončarić N, Peeters FJC, Kroon D, Brummer GJA (2006) Oxygen isotope ecology of recent planktic Foraminifera at the central Walvis Ridge (SE Atlantic). *Paleoceanography*. doi:[10.1029/2005PA001207](https://doi.org/10.1029/2005PA001207)
- Lončarić N, van Iperen J, Kroon D, Brummer GJA (2007) Seasonal export and sediment preservation of diatomaceous, foraminiferal and organic matter mass fluxes in a trophic gradient across the SE Atlantic. *Prog Oceanogr* 73:27–59
- Malmgren BA (1983) Ranking of dissolution susceptibility of planktonic Foraminifera at high latitudes of the South Atlantic Ocean. *Mar Micropaleontol* 8:183–191. doi:[10.1016/0377-8398\(83\)90023-3](https://doi.org/10.1016/0377-8398(83)90023-3)
- Millero FJ, Morse J, Chen CT (1979) The carbonate system in the western Mediterranean Sea. *Deep-Sea Res I* 26:1395–1404
- Milliman JD (1974) *Marine carbonates*. Springer, New York
- Milliman JD (1993) Production and accumulation of calcium carbonate in the ocean: budget of a nonsteady state. *Glob Biogeochem Cycles* 7:927–957
- Milliman JD, Droxler AW (1996) Neritic and pelagic carbonate sedimentation in the marine environment: ignorance is not bliss. *Geol Rundsch* 85:496–504
- Milliman JD, Troy PJ, Balch WM, Adams AK, Li YH, Mackenzie FT (1999) Biologically mediated dissolution of calcium carbonate above the chemical lysocline? *Deep-Sea Res I* 46:1653–1669
- Movellan A (2013) *La biomasse des foraminifères planctoniques actuels et son impact sur la pompe biologique de carbone*. PhD. Thesis, University of Angers
- Naidu PD, Malmgren BA (1996) A high-resolution record of late quaternary upwelling along the Oman margin, Arabian Sea based on planktonic Foraminifera. *Paleoceanography* 11:129–140
- Obata A, Ishizaka J, Endoh M (1996) Global verification of critical depth theory for phytoplankton bloom with climatological in situ temperature and satellite ocean color data. *J Geophys Res* 101:20657–20667
- Parker FL, Berger WH (1971) Faunal and solution patterns of planktonic Foraminifera in surface sediments of the South Pacific. *Deep-Sea Res* 18:73–107. doi:[10.1016/0011-7471\(71\)90017-9](https://doi.org/10.1016/0011-7471(71)90017-9)
- Paull CK, Hills SJ, Thierstein HR (1988) Progressive dissolution of fine carbonate particles in pelagic sediments. *Mar Geol* 81:27–40. doi:[10.1016/0025-3227\(88\)90015-1](https://doi.org/10.1016/0025-3227(88)90015-1)
- Pearson PN (2012) Oxygen isotopes in Foraminifera: overview and historical review. In: Ivany LC, Huber BT (eds) *Reconstructing earth's deep-time climate—the state of the art in 2012*. Paleontological Society Short Course. Paleontological Society Papers, pp 1–38
- Pearson PN, Palmer MR (2000) Atmospheric carbon dioxide concentrations over the past 60 million years. *Nature* 406:695–699
- Peeters F, Ivanova E, Conan S, Brummer GJA, Ganssen G, Troelstra S, van Hinte J (1999) A size analysis of planktic Foraminifera from the Arabian Sea. *Mar Micropaleontol* 36:31–63
- Prell WL, Martin A, Cullen JL, Trend M (1999) The Brown University Foraminiferal Data Base (BFD)
- Ransom B, Shea KF, Burkett PJ, Bennett RH, Baerwald R (1998) Comparison of pelagic and nepheloid layer marine snow: Implications for carbon cycling. *Mar Geol* 150:39–50
- Riebesell U, Gattuso JP, Thingstad TF, Middelburg JJ (2013) Arctic ocean acidification: pelagic ecosystem and biogeochemical responses during a mesocosm study. *Biogeosciences* 10:5619–5626. doi:[10.5194/bg-10-5619-2013](https://doi.org/10.5194/bg-10-5619-2013)
- Rixen T, Haake B, Ittekkot V (2000) Sedimentation in the western Arabian Sea the role of coastal and open-ocean upwelling. *Deep-Sea Res II* 47:2155–2178
- Salter I, Schiebel R, Ziveri P, Movellan A, Lampitt R, Wolff GA (2014) Carbonate counter pump stimulated by natural iron fertilization in the polar frontal zone. *Nat Geosci* 7:885–889. doi:[10.1038/ngeo2285](https://doi.org/10.1038/ngeo2285)
- Sarmiento JL, Gruber N (2006) *Ocean biogeochemical dynamics*. Princeton University Press, Princeton and Oxford
- Sautter LR, Thunell RC (1989) Seasonal succession of planktonic Foraminifera: results from a four-year time-series sediment trap experiment in the Northeast Pacific. *J Foraminif Res* 19:253–267
- Schiebel R (2002) Planktic foraminiferal sedimentation and the marine calcite budget. *Glob Biogeochem Cycles*. doi:[10.1029/2001GB001459](https://doi.org/10.1029/2001GB001459)
- Schiebel R, Hemleben C (2000) Interannual variability of planktic foraminiferal populations and test flux in the eastern North Atlantic Ocean (JGOFS). *Deep-Sea Res II* 47:1809–1852
- Schiebel R, Hemleben C (2005) Modern planktic Foraminifera. *Paläontol Z* 79:135–148
- Schiebel R, Movellan A (2012) First-order estimate of the planktic foraminifer biomass in the modern ocean. *Earth Syst Sci Data* 4:75–89. doi:[10.5194/essd-4-75-2012](https://doi.org/10.5194/essd-4-75-2012)
- Schiebel R, Hiller B, Hemleben C (1995) Impacts of storms on recent planktic foraminiferal test production and CaCO<sub>3</sub> flux in the North Atlantic at 47°N, 20°W (JGOFS). *Mar Micropaleontol* 26:115–129
- Schiebel R, Bijma J, Hemleben C (1997) Population dynamics of the planktic foraminifer *Globigerina bulloides* from the eastern North Atlantic. *Deep-Sea Res I* 44:1701–1713

- Schiebel R, Waniek J, Zeltner A, Alves M (2002) Impact of the Azores front on the distribution of planktic foraminifers, shelled gastropods, and coccolithophorids. *Deep-Sea Res II* 49:4035–4050
- Schiebel R, Barker S, Lendt R, Thomas H, Bollmann J (2007) Planktic foraminiferal dissolution in the twilight zone. *Deep-Sea Res II* 54:676–686
- Schmidt K, De La Rocha CL, Gallinari M, Cortese G (2014) Not all calcite ballast is created equal: differing effects of foraminiferan and coccolith calcite on the formation and sinking of aggregates. *Biogeosciences* 11:135–145. doi:[10.5194/bg-11-135-2014](https://doi.org/10.5194/bg-11-135-2014)
- Scholten JC, Fietzke J, Vogler S, Rutgers van der Loeff MM, Mangini A, Koeve W, Waniek J, Stoffers P, Antia A, Kuss J (2001) Trapping efficiencies of sediment traps from the deep Eastern North Atlantic: the  $^{230}\text{Th}$  calibration. *Deep-Sea Res II* 48:2383–2408. doi:[10.1016/S0967-0645\(00\)00176-4](https://doi.org/10.1016/S0967-0645(00)00176-4)
- Sexton PF, Wilson PA, Pearson PN (2006) Microstructural and geochemical perspectives on planktic foraminiferal preservation: “Glassy” versus “Frosty”. *Geochem Geophys Geosystems*. doi:[10.1029/2006GC001291](https://doi.org/10.1029/2006GC001291)
- Siegel DA, Deuser WG (1997) Trajectories of sinking particles in the Sargasso Sea: modeling of statistical funnels above deep-ocean sediment traps. *Deep-Sea Res I* 44:1519–1541
- Simstich J, Sarnthein M, Erlenkeuser H (2003) Paired  $\delta^{18}\text{O}$  signals of *Neogloboquadrina pachyderma* (s) and *Turborotalita quinqueloba* show thermal stratification structure in Nordic Seas. *Mar Micropaleontol* 48:107–125
- Stow DAV, Pudsey CJ, Howe JA, Faugeres JC, Viana AR (2002) Deep-water contourite systems: modern drifts and ancient series, seismic and sedimentary characteristics. In: *Geological Society Memoir* 22. Geological Society of London, London, p 464
- Takahashi K, Bé AWH (1984) Planktonic Foraminifera: factors controlling sinking speeds. *Deep-Sea Res Part Oceanogr Res Pap* 31:1477–1500
- Thiel H, Pfannkuche O, Schriever G, Lochte K, Gooday AJ, Hemleben C, Mantoura RFG, Turley CM, Patching JW, Riemann F (1989) Phytodetritus on the deep-sea floor in a central oceanic region of the Northeast Atlantic. *Biol Oceanogr* 6:203–239. doi:[10.1080/01965581.1988.10749527](https://doi.org/10.1080/01965581.1988.10749527)
- Thunell RC, Honjo S (1987) Seasonal and interannual changes in planktonic foraminiferal production in the North Pacific. *Nature* 328:335–337
- Turley CM, Stutt ED (2000) Depth-related cell-specific bacterial leucine incorporation rates on particles and its biogeochemical significance in the Northwest Mediterranean. *Limnol Oceanogr* 45:419–425
- Van Aken HM (2000) The hydrography of the mid-latitude Northeast Atlantic Ocean: II: the intermediate water masses. *Deep-Sea Res I* 47:789–824
- Van Raden UJ, Groeneveld J, Raitzsch M, Kucera M (2011) Mg/Ca in the planktonic Foraminifera *Globorotalia inflata* and *Globigerinoides bulloides* from Western Mediterranean plankton tow and core top samples. *Mar Micropaleontol* 78:101–112. doi:[10.1016/j.marmicro.2010.11.002](https://doi.org/10.1016/j.marmicro.2010.11.002)
- Van Sebille E, Scussolini P, Durgadoo JV, Peeters FJC, Biastoch A, Weijer W, Turney C, Paris CB, Zahn R (2015) Ocean currents generate large footprints in marine palaeoclimate proxies. *Nat Commun* 6:6521. doi:[10.1038/ncomms7521](https://doi.org/10.1038/ncomms7521)
- Vincent E, Berger WH (1981) Planktonic Foraminifera and their use in paleoceanography. *Ocean Lithosphere Sea* 7:1025–1119
- Volbers ANA, Henrich R (2002) Present water mass calcium carbonate corrosiveness in the eastern South Atlantic inferred from ultrastructural breakdown of *Globigerina bulloides* in surface sediments. *Mar Geol* 186:471–486. doi:[10.1016/S0025-3227\(02\)00333-X](https://doi.org/10.1016/S0025-3227(02)00333-X)
- Von Gyldenfeldt AB, Carstens J, Meincke J (2000) Estimation of the catchment area of a sediment trap by means of current meters and foraminiferal tests. *Deep-Sea Res II* 47:1701–1717
- Wefer G (1989) Particle flux in the ocean: effects of episodic production. In: Berger WH, Smetacek VS, Weger G (eds) *Productivity of the ocean: present and past*. Dahlem Workshop Proceedings, pp 139–154
- Wejnert KE, Pride CJ, Thunell RC (2010) The oxygen isotope composition of planktonic Foraminifera from the Guaymas Basin, Gulf of California: seasonal, annual, and interspecies variability. *Mar Micropaleontol* 74:29–37
- Weyl PK (1978) Micropaleontology and ocean surface climate. *Science* 202:475–481
- Žarić S, Schulz M, Mulitza S (2006) Global prediction of planktic foraminiferal fluxes from hydrographic and productivity data. *Biogeosciences* 3:187–207
- Zeebe RE (2012) History of seawater carbonate chemistry, atmospheric  $\text{CO}_2$ , and ocean acidification. *Annu Rev Earth Planet Sci* 40:141–165
- Zeebe RE, Wolf-Gladrow D (2001)  $\text{CO}_2$  in Seawater: equilibrium, Kinetics. *Isotopes*, Elsevier, Amsterdam